UC Berkeley
Research Reports

Title
Traffic Data Measurement and Validation

Permalink
https://escholarship.org/uc/item/72t619n7

Author
Coifman, Benjamin

Publication Date
2001-12-01

eScholarship.org Powered by the California Digital Library
University of California

CALIFORNIA PATH PROGRAM
INSTITUTE OF TRANSPORTATION STUDIES
UNIVERSITY OF CALIFORNIA, BERKELEY

Traffic Data Measurement and Validation

Benjamin Coifman
The Ohio State University

California PATH Research Report
UCB-ITS-PRR-2001-40

This work was performed as part of the California PATH Program of the University of California, in cooperation with the State of California Business, Transportation, and Housing Agency, Department of Transportation; and the United States Department of Transportation, Federal Highway Administration.

The contents of this report reflect the views of the authors who are responsible for the facts and the accuracy of the data presented herein. The contents do not necessarily reflect the official views or policies of the State of California. This report does not constitute a standard, specification, or regulation.

Final Report for MOU 3000

December 2001

ISSN 1055-1425

Traffic Data Measurement and Validation

MOU 3000 Final Report

Benjamin Coifman

Civil Engineering

470 Hitchcock Hall

The Ohio State University

Columbus, OH 43210

phone: (614) 292-4282

fax: (614) 292-3780

email: Coifman.1@OSU.edu

1 OVERVIEW

Caltrans collects traffic data for many monitoring and control applications and the ultimate goal of the traffic surveillance system is to provide accurate data to these high level applications. The surveillance system includes data measurement, averaging and verification algorithms. This report presents improvements to many elements of the surveillance system. First, section 2 addresses many shortcomings in average speed estimation at single loop detectors, as well as other sensors that estimate speed from average flow and occupancy. At the root of these problems is the fact that the conventional estimation methodology assumes a fixed vehicle length. It is shown that this assumption does not hold for many samples, both because the true average vehicle length can change throughout the day and because a given sample may not be representative of an average sample. Next, section 3 presents a more accurate method to estimate velocity at single loop detectors. It is shown that this method approaches the accuracy of velocity measurements from dual loop detectors. This new approach does not eliminate the benefit of dual loops, section 4 presents a new method to estimate link travel time from measurements recorded at a dual loop detector. The estimates are very close to the true travel times and it is shown that when estimation errors do occur, they can usually be identified. Finally, experience by Caltrans shows that there is a need to develop and deploy more sophisticated error detection and data verification algorithms. Section 5 presents eight new detector validation tests using data on individual vehicles, i.e., event data.

2 IMPROVED VELOCITY ESTIMATION USING SINGLE LOOP DETECTORS

2.1 Introduction

Loop detectors are the preeminent vehicle detector for freeway traffic surveillance. They are frequently deployed as single detectors, i.e., one loop per lane per detector station. Although single loops have been used for decades, debate continues on how to interpret the measurements and how to calibrate the detectors. In conventional practice, the single loop measurements are very noisy and many researchers have sought sophisticated filtering methods, e.g., Mikhalkin et al. (1972), Pushkar et al. (1994), and Dailey (1999). Unfortunately, most of the preceding efforts focused on complicated models without explicitly identifying the sources of error. The earlier works also lose sight of the end goal: to produce an algorithm that can be deployed on a simple processor, such as a Model 170 controller.

This section provides a new perspective by clarifying the source of several errors and suggesting ways to reduce the impacts. The body of this work emphasizes velocity estimation, but it has implications for tests of detector data quality as well. The first subsection reviews the state of the practice for parameter measurement and estimation from single loop detectors. The next subsection illustrates how conventional practice may be susceptible to changes in the vehicle population throughout the day as well as errors due to sample size. The section continues by developing an algorithm to overcome these problems. Finally, the discussion shows how the work has implications for tests of detector data quality and elucidates the findings of an earlier study that concluded that single loop velocity estimates are biased.

2.2 Parameter Measurement and Estimation

Conventional single loop detectors are capable of measuring flow, the number of vehicles that pass the detector during a fixed sample period, and occupancy, the percentage of the given

sample period that the detector is "occupied" by vehicles. For each lane, these two parameters are defined as:

$$q_k = \frac{n_k}{T} \tag{2-1A}$$

$$\theta_k = \frac{\sum_{j \in J_k} t_j}{T} \tag{2-1B}$$

where the subscript "k" indicates the given sample, subscript "j" indicates vehicle specific parameters and

q_k = flow during sample k

θ_k = occupancy during sample k

n_k = number of vehicles that pass the detector during sample k

T = sampling period

J_k = set of all vehicles that pass the detector during sample k

t_j = vehicle j's *on time*.

Two interdependent vehicle parameters are of interest for estimating mean sample velocity: vehicle velocity and vehicle length. The relationship between these two parameters for a vehicle passing over a loop detector is simply:

$$L_j = L_j^v + L_j^s = v_j \cdot t_j \tag{2-2}$$

where

L_j = vehicle j's effective length as "seen" by the detector

L_j^v = vehicle j's true length

L_j^s = length of detector's sensitivity region for vehicle j

v_j = vehicle j's velocity

The length of the detector's sensitivity region typically depends on many variables such as the vehicle's position in the lane, height of the vehicle's underframe, and the amount of ferrous metal in the vehicle. It is difficult to separate this length from the vehicle's true length using loop detector data, so for the rest of this document "length" will refer to the sum of these two lengths, often referred to as the effective vehicle length.

From equations 2-1 and 2-2,

$$\theta_k = \frac{1}{T}\sum_{j\in J_k}\frac{L_j}{v_j} = q_k \cdot \frac{1}{n_k}\sum_{j\in J_k}\frac{L_j}{v_j} \tag{2-3A}$$

assuming that individual vehicle lengths and velocities are uncorrelated,

$$\theta_k \approx \frac{q_k \cdot \overline{L}_k}{\overline{v}_k} \tag{2-3B}$$

where

$\overline{L}_k$ = arithmetic mean vehicle length for sample k

$\overline{v}_k$ = harmonic mean vehicle velocity for sample k, often referred to as the *space mean speed*.

In other words,

$$\overline{v}_k \approx \frac{q_k \cdot \overline{L}_k}{\theta_k} \tag{2-4}$$

Equation 2-4 shows the relationship between mean velocity and mean length, but these two parameters can not be measured independently at a single loop. Typically, an operating agency will use one of two approaches to address this problem. In the first case, $\overline{L}_k$ is simply set to a constant value, $\hat{L}$, and Equation 2-5 is used to estimate $\overline{v}_k$:

$$\hat{v}_k = \frac{q_k \cdot \hat{L}}{\theta_k} \tag{2-5}$$

There are many site specific variables that can influence the mean vehicle length, such as the percentage of long vehicles in the lane and the detector's sensitivity. So, other operating agencies assume a fixed free flow velocity and reversing the assignment in Equation 2-5, estimate $\hat{L}$ each day during periods when traffic over the detector is almost certain to be free flowing. Then, $\hat{L}$ is held fixed during the remainder of the day and the velocity estimation progresses using Equation 2-5 directly.

2.3 Analysis

Some of the site specific variables are corrected with a daily estimate of $\hat{L}$, but other factors are not addressed, such as the possibility that the percentage of long vehicles may change during the day or the simple fact that a sample with few vehicles (i.e., low flow) may not have a representative sample of vehicle lengths. For this study, we examine 24 hours of detector actuations, sampled at 60 Hz, for each lane at a detector station on Interstate-80 in Berkeley, California. The data come from dual loop detectors. In this configuration, it is possible to measure true vehicle velocities by dividing the loop separation by the difference in arrival times at each loop. Finally, $\overline{L}_k$ is calculated using Equation 2-4 by assuming absolute equality.

Figure 2-1A illustrates the time series evolution of $\overline{L}_k$ for the eastbound traffic with $T = 15\,\text{min}$. Following Caltrans convention, lanes are numbered starting at the inside and increasing outward. The legend indicates the total number of vehicles in each lane during the day. Including the westbound data (not shown), the observed values of $\overline{L}_k$ range from 19 feet to 51 feet and almost all lanes exhibit a strong temporal dependency. Figure 2-1B-C show the corresponding n_k and $\overline{v}_k$, respectively.

When an operating agency estimates $\hat{L}$, they typically sample the value during early morning hours. As one would expect, these hours are free flowing for this example; however, they also correspond to the highest values of $\overline{L}_k$ and lowest values of q_k. Thus, if $\hat{L}$ were estimated strictly during the early morning, estimates of velocity from Equation 2-5 would be too high throughout the remainder of the day. Since the phenomena depend on site specific factors, the figures indicate the need for an improved method of estimating $\hat{L}$ on-line.

Figure 2-2 shows the cumulative distribution of $\overline{L}_k$ for the eastbound lanes using four different sampling periods. Although Lane 1 shows little variance due to a truck restriction, the other lanes exhibit a large variance. So no single value of $\hat{L}$ will be representative of all samples and a value of $\hat{L}$ estimated using one value of T might not be valid for another value of T.

The primary source of this variance comes from the fact that the vehicles observed during a given sample may not be "typical". Figure 2-3 shows the observed distribution of individual vehicle lengths for the eastbound traffic. Approximately 85 percent of the vehicles are between 15 and 22 feet, but some are as long as 80 feet or roughly four times the median length. When n_k is small, i.e., low flow, a long vehicle can skew θ_k simply because it takes more time for the long vehicle to pass the detector.

In accordance with the law of large numbers, the sample distribution should become more representative of the entire population as n_k increases, which in turn, increases with q_k and T. Figure 2-4 illustrates this phenomena using the eastbound data from all lanes for three values of T. The top half of the figure shows $\overline{L}_k$ during free flow conditions, $\overline{v}_k$ > 50 mph, while the lower half shows $\overline{L}_k$ during congestion, $\overline{v}_k$ < 50 mph. In parts A and D, where $T = 30\,\text{sec}$, the maximum number of vehicles per sample is so small that the observations fall into distinct columns, i.e., the first column contains observations with only one vehicle, the second column contains observations with only two vehicles, and so on. Notice that for each T, the range of $\overline{L}_k$

decreases as q_k increases; also note that in this data set, the lowest flows are only observed during free flow conditions.

2.3.1 Improving the Length Estimates

As previously noted, a single loop detector can not measure $\bar{v}_k$ directly and estimates of $\hat{L}$ may be biased by the time of day. To overcome these problems, $\hat{L}$ is estimated during periods when the traffic should be free flowing. Rather than choosing a period of the day a priori, the data are used to make the distinction. Empirically, free flow conditions correspond to low occupancies and Equation 2-3B explicitly shows that θ_k is inversely proportional to $\bar{v}_k$. For this study, a sample is considered free flowing if

$$\theta_k < \theta_{threshold} \tag{2-6}$$

where $\theta_{threshold}$ was set to 10 percent. The value was chosen so that most free flow samples would be selected, but low enough to ensure that very few (if any) congested samples are selected. In practice, this threshold could be set from a plot of flow versus occupancy. To account for samples with high θ_k due to free flowing trucks, for $T = 30\,\text{sec}$, a sample is also considered free flowing if at least half of the 10 preceding samples satisfy Equation 2-6. Next,

$$\hat{L} = v_{ff} \cdot mean\left(\frac{\theta_k}{q_k}\right) \forall k \in K \tag{2-7}$$

where

v_{ff} = assumed fixed free flow velocity, set to 60 mph for this study

K = set of all free flow samples with $q_k > 0$ and $\theta_k > 0$ in the given lane during the 24 hour study.

The resulting $\hat{L}$ for the eastbound traffic are shown in Table 2-1. Using these values and Equation 2-5 to calculate $\hat{v}_k$, Figure 2-5 shows $\hat{v}_k$ versus $\overline{v}_k$ over entire 24 hour study. The solid line in each plot indicates where the estimated values equal the measured values. Note that $\hat{v}_k$ ranges between 20 mph and 120 mph for samples with $\overline{v}_k$ > 50 mph. In other words, the estimate is very noisy when the traffic is free flowing. The noise is primarily due to the variance in $\overline{L}_k$ at low flow (recall from Equations 2-4 and 2-5, $\hat{v}_k \approx \overline{v}_k \cdot \hat{L}/\overline{L}_k$). Finally, consider the congested observations, $\overline{v}_k$ < 50 mph. In each lane the observations are roughly collinear and the guess of v_{ff} serves as a scaling factor, increasing or decreasing the slope of the congested data. In lane 1, the guess of v_{ff} was too low and the estimated velocities are lower than the measured velocities, while in lanes 3 and 4, the opposite is true. This error is included in the plots because it can not be eliminated from single loop detector data without additional detectors.

The analysis is repeated with $T = 5\,\text{min}$ to reduce the estimate noise. Now, however, a sample is only considered free flowing if it satisfies Equation 2-6 or the preceding sample satisfied Equation 2-6. Once more the resulting $\hat{L}$ are shown in Table 2-1, while Figure 2-6 shows $\hat{v}_k$ versus $\overline{v}_k$ for $T = 5\,\text{min}$. Even with the longer sampling period, the estimates are still noisy when the traffic is free flowing.

To illustrate the effects of different values of v_{ff} or $\hat{L}$, consider the percent error in $\hat{v}_k$ relative to $\overline{v}_k$ over the entire day for various fixed values of $\hat{L}$. Figure 2-7 shows contour plots of the percent error as $\hat{L}$ ranges between 16 and 32 feet for two different lanes when $T = 30\,\text{sec}$ and $T = 5\,\text{min}$. For example, when $\hat{L}$ = 19 feet in Figure 2-7A, approximately 70 percent of the estimated velocities are within 5 percent of the measured values. Comparing the top plot to the bottom plot in either lane, the longer sampling period increases n_k and thus, reduces the error. Notice that the optimal value of $\hat{L}$ appears to depend on T in the right-hand plots (lane 5 westbound), reaffirming the fact that $\hat{L}$ estimated at one value of T may not be valid for another

value of T. The figure also shows that performance is relatively stable for length estimates within a few feet of the optimal value.

2.3.2 Improving the Velocity Estimates

Free flow velocity estimates are poor during low flow, but from an operational standpoint, it is sufficient to know that traffic is free flowing during these conditions. This supposition is implicit with on-line estimation of $\hat{L}$. Once more, exploiting the fact that free flow, low flow samples are characterized by low occupancy, the estimated velocity can be set to a constant value, $\hat{v}_k = v_{ff}$ when $\theta_k < \theta_{threshold}$. Rewriting Equation 2-5 to include this constraint:

$$\hat{v}_k = \begin{cases} \dfrac{q_k \cdot \hat{L}}{\theta_k}, & \theta_k \geq \theta_{threshold} \\ v_{ff}, & \theta_k < \theta_{threshold} \end{cases} \tag{2-8}$$

To illustrate the benefits of this constraint, return to the data in Figure 2-6. Recalculating $\hat{v}_k$ using Equation 2-8 with $\theta_{threshold} = 10\%$, the new relationships are shown in Figure 2-8. Notice that almost all of the noise has been eliminated from the estimates corresponding to samples with $\bar{v}_k > 50$ mph. Figure 2-9 compares the time series $\hat{v}_k$ from Equation 2-5, $\hat{v}_k$ from Equation 2-8, and $\bar{v}_k$. In this figure, one can see that Equation 2-8 removed many erroneous velocity estimates, particularly during the early morning. Applying Equation 2-8 to the 30 second data yields similar results, as shown in Figure 2-10.

2.4 Implementation

The analysis for $T = 30\,\text{sec}$ used a moving average to identify free flow periods with high θ_k, but a moving average is memory intensive. In contrast, exponential filtering can accomplish the same goal with almost no data storage. The following pseudo-code can be used to implement the method presented above:

if $\theta_k > 0$ and $q_k > 0$

if $\theta_k < 10\%$ or $u > 0.1$

$$\hat{L} = v_{ff} \cdot mean\left(\frac{\theta_k}{q_k}\right) \cdot r + \hat{L} \cdot (1 - r)$$

$$\hat{v}_k = v_{ff}$$

$$u = 1 \cdot p + u \cdot (1 - p)$$

else

$$\hat{v}_k = \frac{q_k \cdot \hat{L}}{\theta_k}$$

$$u = 0 \cdot p + u \cdot (1 - p)$$

end

end

where

r = filtering factor with a time constant on the order of a week (to minimize the time of day dependency illustrated in Figure 2-1A), e.g., $r = 1/20000$ for $T = 30\,\text{sec}$ and $r = 1/2000$ for $T = 5\,\text{min}$.

p = filtering factor with a time constant on the order of 5 minutes, e.g., $p = 0.2$ for $T = 30\,\text{sec}$ and $p = 1$ for $T = 5\,\text{min}$.

u = an indicator variable used in conjunction with p to determine whether preceding samples were free flowing.

Rather than using a static assignment of $\hat{L}$, as in Equation 2-7, the algorithm uses an exponential filter to dynamically update $\hat{L}$. This pseudo-code is presented to show that the method can be implemented easily, but it is left to future research to determine the optimal implementation.

2.5 Discussion

2.5.1 Implications Beyond Single Loop Velocity Estimates

The impact of this work to single loop detectors is straightforward, but this work has implications for dual loop detectors as well. Earlier studies have developed automated tests of detector data quality, e.g., Jacobson et al. (1990), Cleghorn et al. (1991), and Nihan (1997). Their goal is to eliminate erroneous measurements due to transient problems or component failures. Similar systems often go undocumented in the literature because they are either designed in-house by an operating agency or a consulting firm (see Chen and May, 1987, for examples). Most of these data quality tests can be expressed using the following constraint to bound *good* dual loop data:

$$\bar{v}_k \in \left[\frac{q_k \cdot L_{\min}\left(q_k, \bar{v}_k, \theta_k\right)}{\theta_k}, \frac{q_k \cdot L_{\max}\left(q_k, \bar{v}_k, \theta_k\right)}{\theta_k} \right] \tag{2-9A}$$

where $L_{\min}$ and $L_{\max}$ are lower and upper bounds, respectively, that may depend on q_k, $\bar{v}_k$ or θ_k. Naturally, this constraint reduces to the following for single loop detector data:

$$\hat{v}_k \in \left[\frac{q_k \cdot L_{\min}\left(q_k, \theta_k\right)}{\theta_k}, \frac{q_k \cdot L_{\max}\left(q_k, \theta_k\right)}{\theta_k} \right] \tag{2-9B}$$

Some of these tests fail to accommodate the fact that the variance in $\bar{L}_k$ increases as q_k decreases. The author recently identified such a system currently in use by a large operating agency. In particular, the agency applied Equation 2-9A, using fixed values of $L_{\min}$ and $L_{\max}$, to dual loop data. The test discarded almost all early morning observations from the agency's 400 detector stations simply because the constraint is too restrictive during low occupancy conditions.

2.5.2 Previous Research in the Context of the new Analysis

There has been some confusion in the discipline since Hall and Persaud (1989) concluded that, for a fixed value of $\hat{L}$, Equation 2-5 does not hold over an extended range of occupancies. Their paper examined the "g-factor" which is simply the inverse of $\hat{L}$, and the analysis used,

$$g = \frac{1}{\overline{L}_k} \tag{2-10}$$

Roughly summarizing their plots of g versus occupancy: g decreases by a factor of two from one percent to five percent occupancy, remains constant over the range of five percent to 40 percent occupancy, and then drops by an order of magnitude from 40 percent to 80 percent occupancy. To reduce errors due to vehicle lengths, they selected lanes with truck restrictions. In an attempt to reproduce these results, Figure 2-11A shows the g-factor versus occupancy for lane 1 eastbound. The g-factor does not exhibit the predicted occupancy dependence. There is one difference, however, the earlier study used occupancy expressed in integer percent. After truncating percent occupancy to integer values and recalculating g, Figure 2-11B shows the new g-factor versus integer percent occupancy. This plot exhibits the non-linearity at low occupancies predicted by Hall and Persaud, but it does not show the drop in g at high occupancy. Finally, using *time mean speed*[1] rather than *space mean speed* and the truncated occupancy to calculate g, Figure 2-11C follows the predictions from the earlier study. Figure 2-12 compares the various methods of calculating the g-factor. It shows mean g-factor over one percent ranges up to 35 percent occupancy and then over five percent ranges through 50 percent occupancy. Note that by using *time mean speed* without truncating occupancy, the g-factor follows the predictions for high occupancy but it does not follow the predictions for low occupancy.

[1] The arithmetic mean of each samples' vehicle velocities.

These figures clearly show that subtle differences in aggregation can lead to significant differences in parameter relationships. The tools and data necessary for this detailed analysis were not available to researchers when Hall and Persaud published their work. Although their diagnosis seems to be incorrect, Hall and Persaud correctly identified a significant problem with conventional velocity estimation. An operating agency should expect to encounter similar round-off errors at low occupancy if they use truncated occupancy to estimate $\hat{L}$ and this error will propagate to all subsequent velocity estimates. In the course of their analysis, Hall and Persaud assumed the operating agency was measuring *space mean speed* when in fact it appears that the agency was measuring *time mean speed*. This measurement error would explain their results at high occupancy. To prevent such oversights in the future, researchers should learn the subtle details of the data measurement and aggregation procedures underlying their detector data. One must remember that loop detectors, as well as most other vehicle detectors, are not precision instruments. To keep the detectors affordable, they are typically designed to meet existing operational needs with minimal excess performance. Finally, recall that the results in Figure 2-12 represent a lane with a truck restriction. As shown earlier in this section, when trucks are present, the large range of possible vehicle lengths will reduce the accuracy of velocity estimates from single loops.

2.6 Conclusions

The significance of this work to single loop detectors is straightforward. Figure 2-7 shows that no single estimate of $\hat{L}$ is appropriate for all samples; but fortunately, for most samples, it is sufficient for the estimate to be within a few feet of the optimal value. Significant errors occur at low flows, however, since the variance in $\overline{L}_k$ increases as q_k decreases. This variance degrades the velocity estimation because $\overline{L}_k$ is less likely to be *average*, as shown in Figure 2-4. Exploiting the fact that the low flow free flow samples are characterized by low occupancy, this section has shown that it is possible to identify these conditions and simply report that traffic is

free flowing (Figures 2-9 and 2-10). This section has presented improved methods for estimating $\hat{L}$ and $\hat{v}_k$ incorporating these findings. Unlike many preceding works, the approach is simple enough that it can be implemented on existing traffic controllers that have limited processing power, such as a Model 170 controller. Although the implementation is fairly simple, this work has wide ranging implications for practitioners and researchers. For example, the discussion shows how the work is applicable to automated tests of detector data quality, both from dual and single loop detectors. Then, the section closes by refuting an earlier study, showing that in the presence of a truck restriction, the use of a single estimate $\hat{L}$ in Equation 2-5 is indeed valid over an extended range of occupancies provided care is taken to measure the right parameters and prevent round-off errors.

Figure 2-1, (A) True $\overline{L}_k$ by lane as a function of time for the eastbound lanes on a single day, T = 15 minutes, and the corresponding (B) number of vehicles per sample (C) measured velocities.

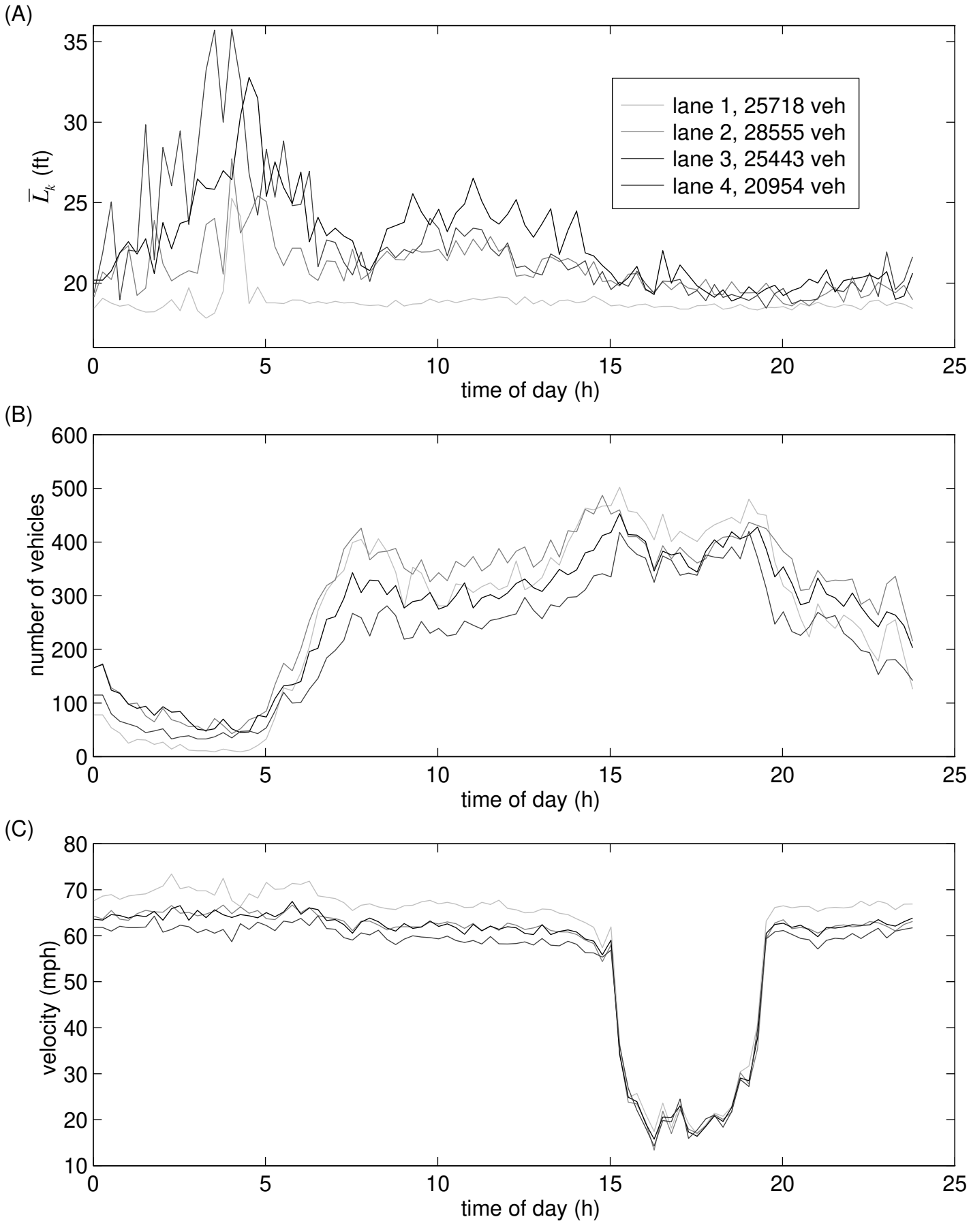

Figure 2-2, Cumulative distribution of the true $\overline{L}_k$ over 24 hours for the eastbound traffic, (A) lane 1 (B) lane 2 (C) lane 3 (D) lane 4.

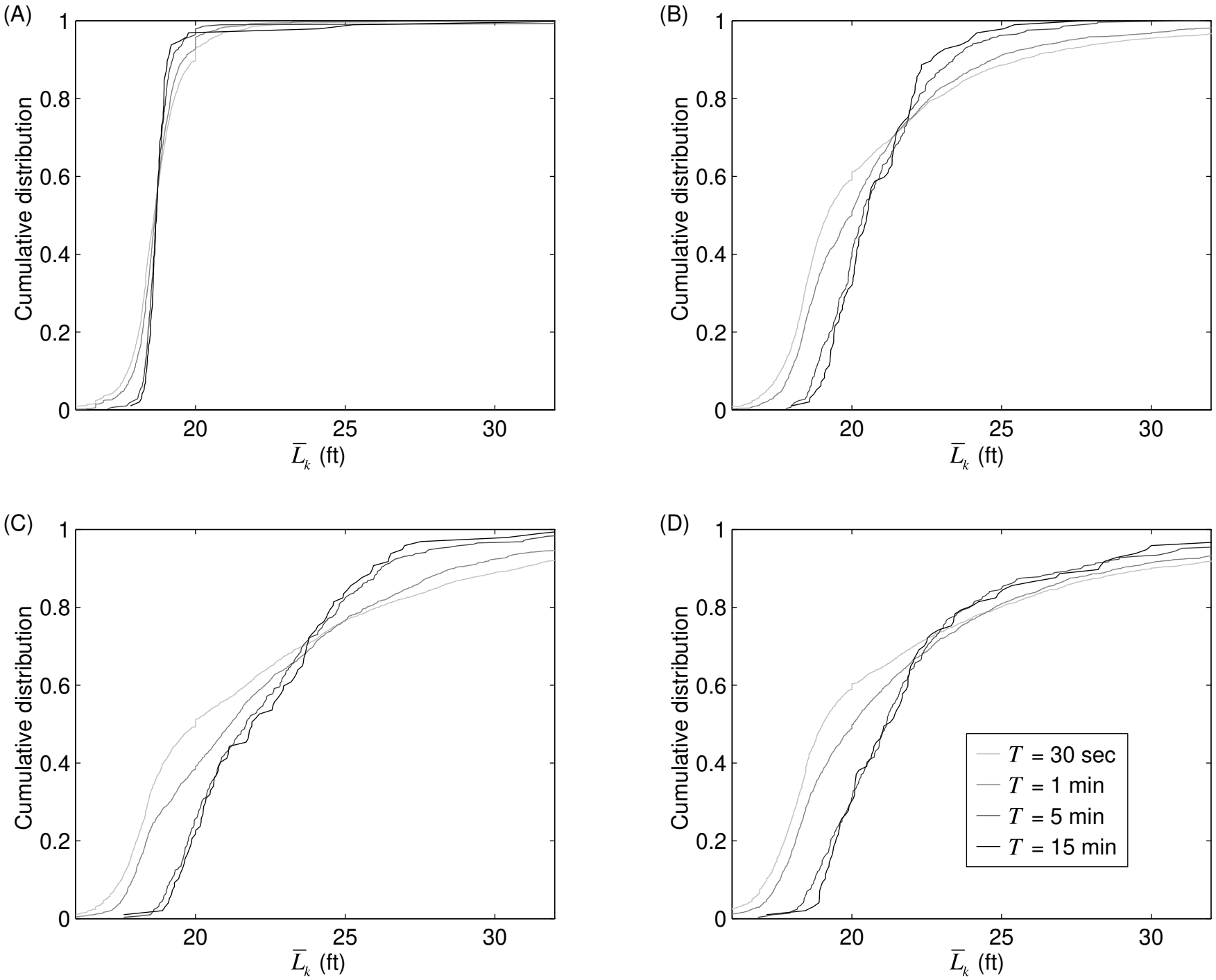

Figure 2-3, (A) Cumulative distribution of individual vehicle lengths, L_j, for the eastbound lanes, (B) detail of part A.

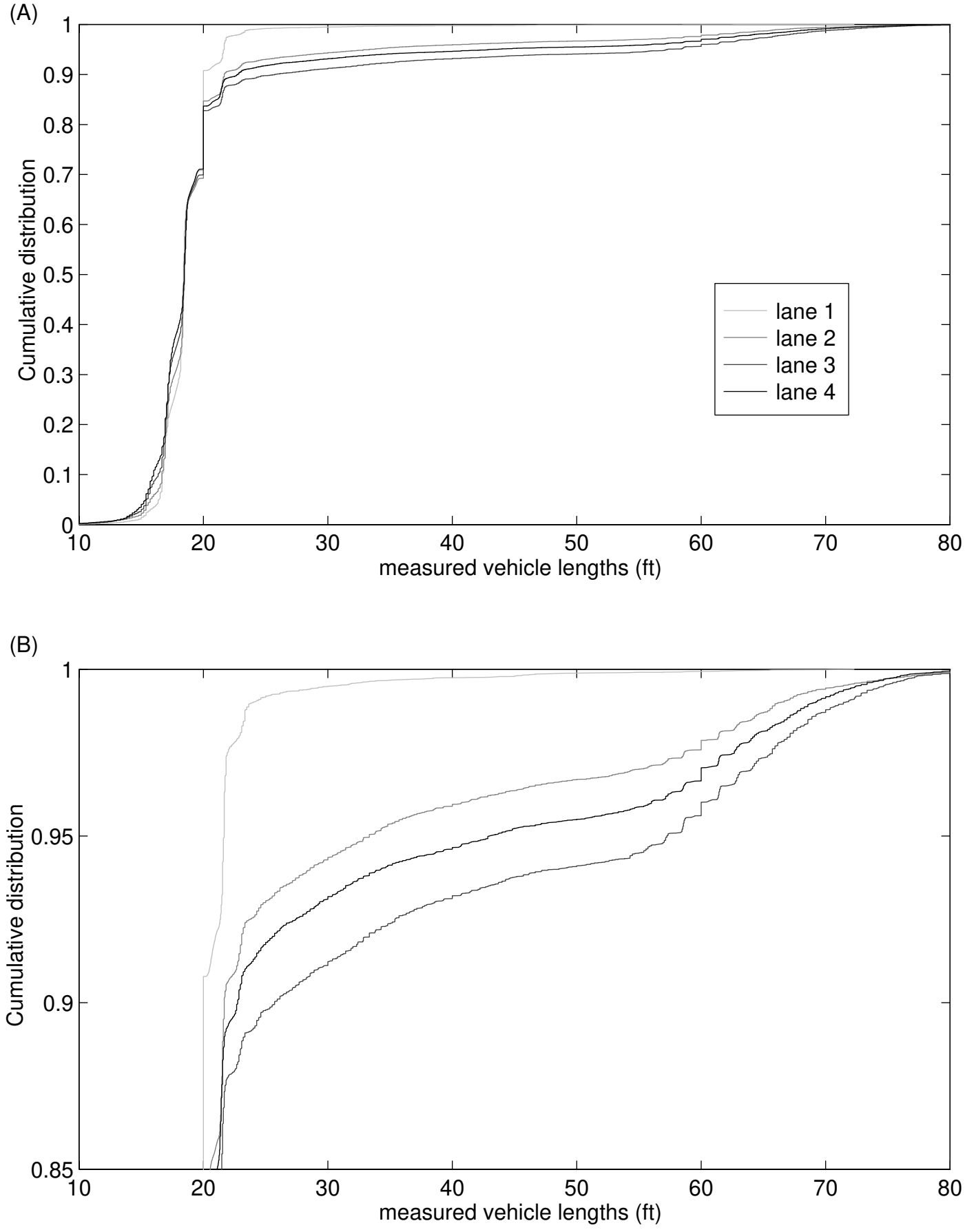

Figure 2-4, $\overline{L}_k$ versus flow, q_k, for the eastbound traffic: (A)-(C) during free flow, $\overline{v}_k$ > 50 mph and (D)-(F) congestion, $\overline{v}_k$ < 50 mph; sampled at (A) & (D) T = 30 sec, (B) & (E) T = 5 min, (C) & (F) T = 15 min.

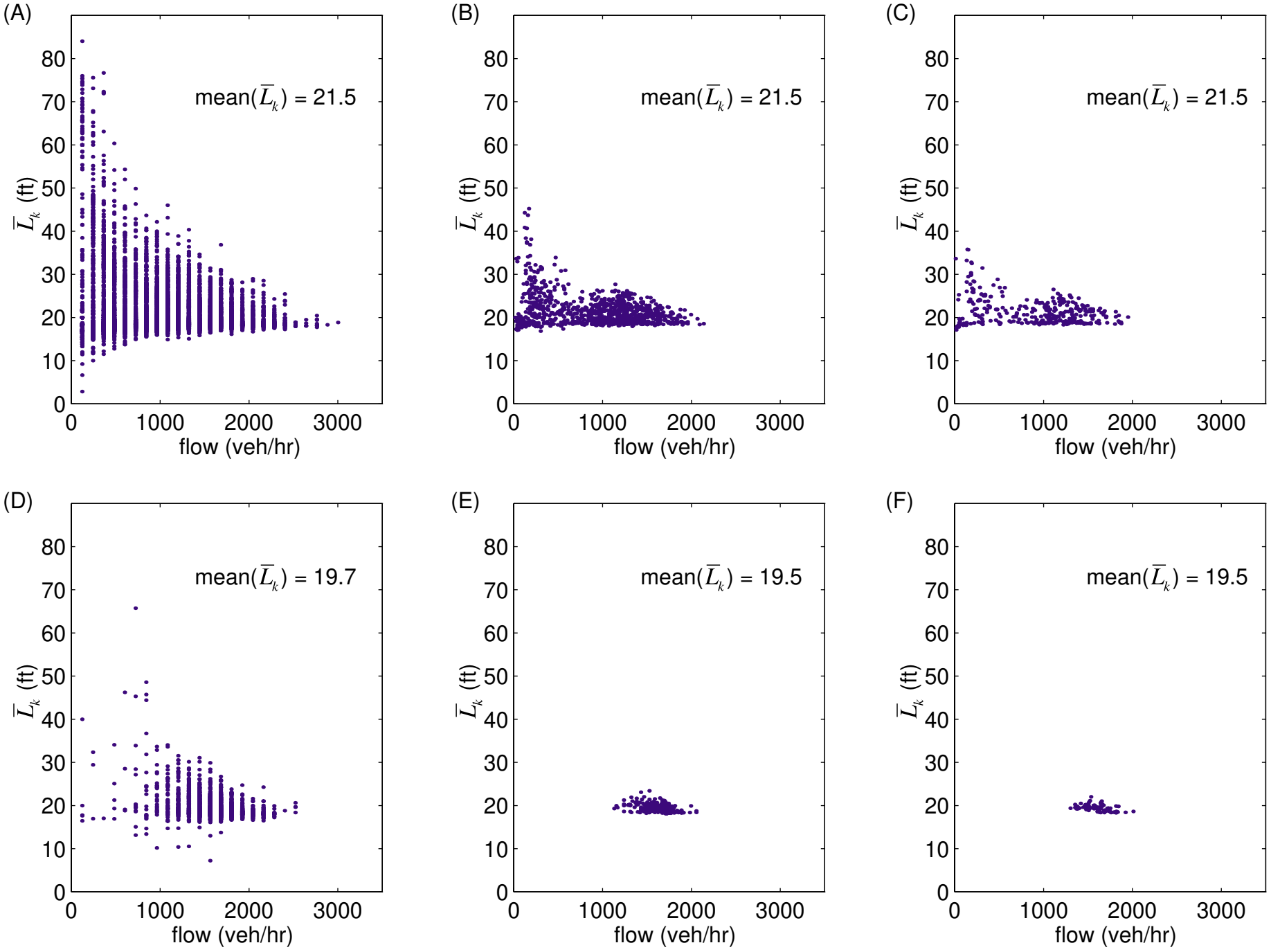

Figure 2-5, Estimated velocity versus measured velocity, eastbound traffic, T = 30 sec, (A) lane 1, (B) lane 2, (C) lane 3, (D) lane 4.

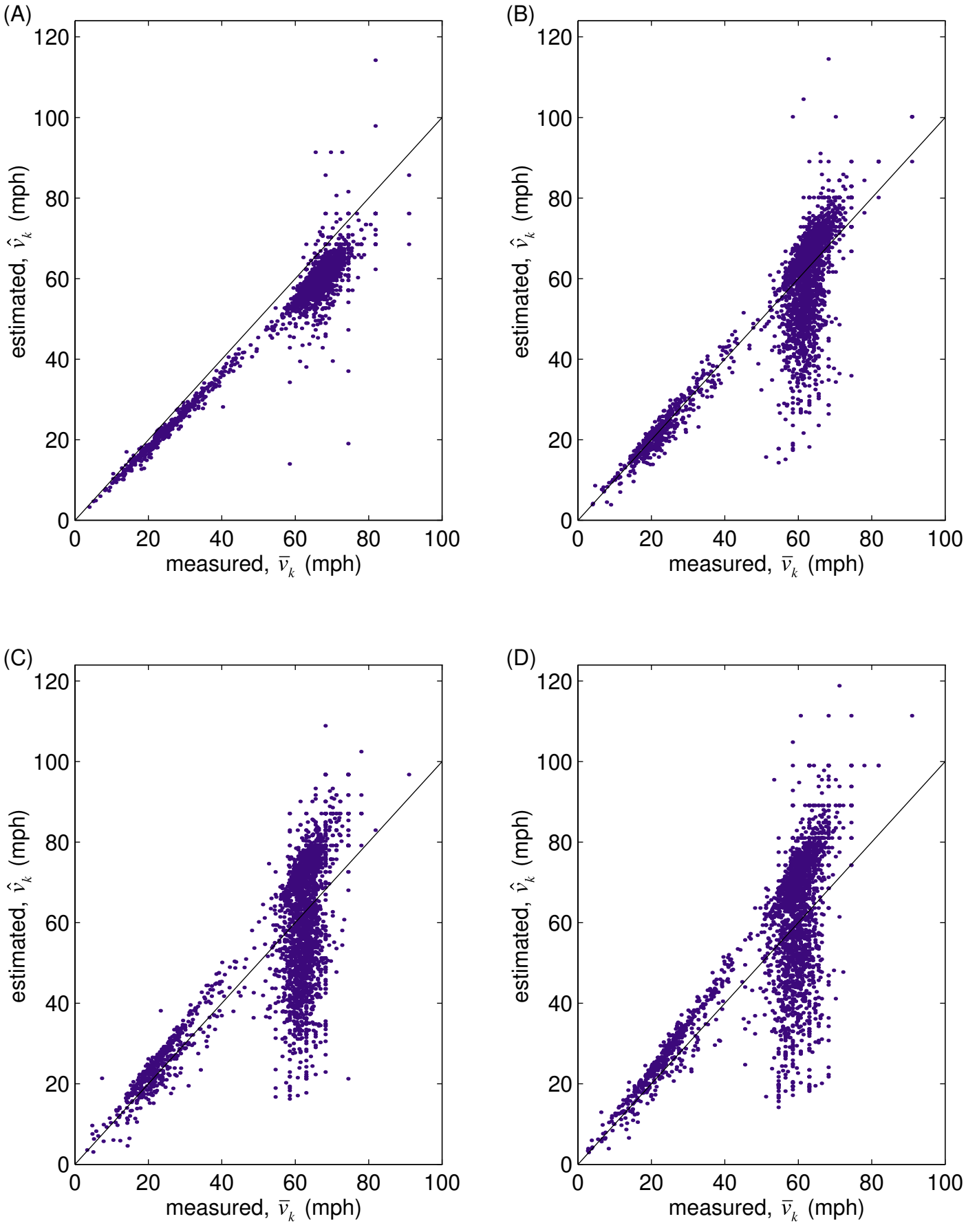

Figure 2-6, Estimated velocity versus measured velocity, eastbound traffic, T = 5 min, (A) lane 1, (B) lane 2, (C) lane 3, (D) lane 4.

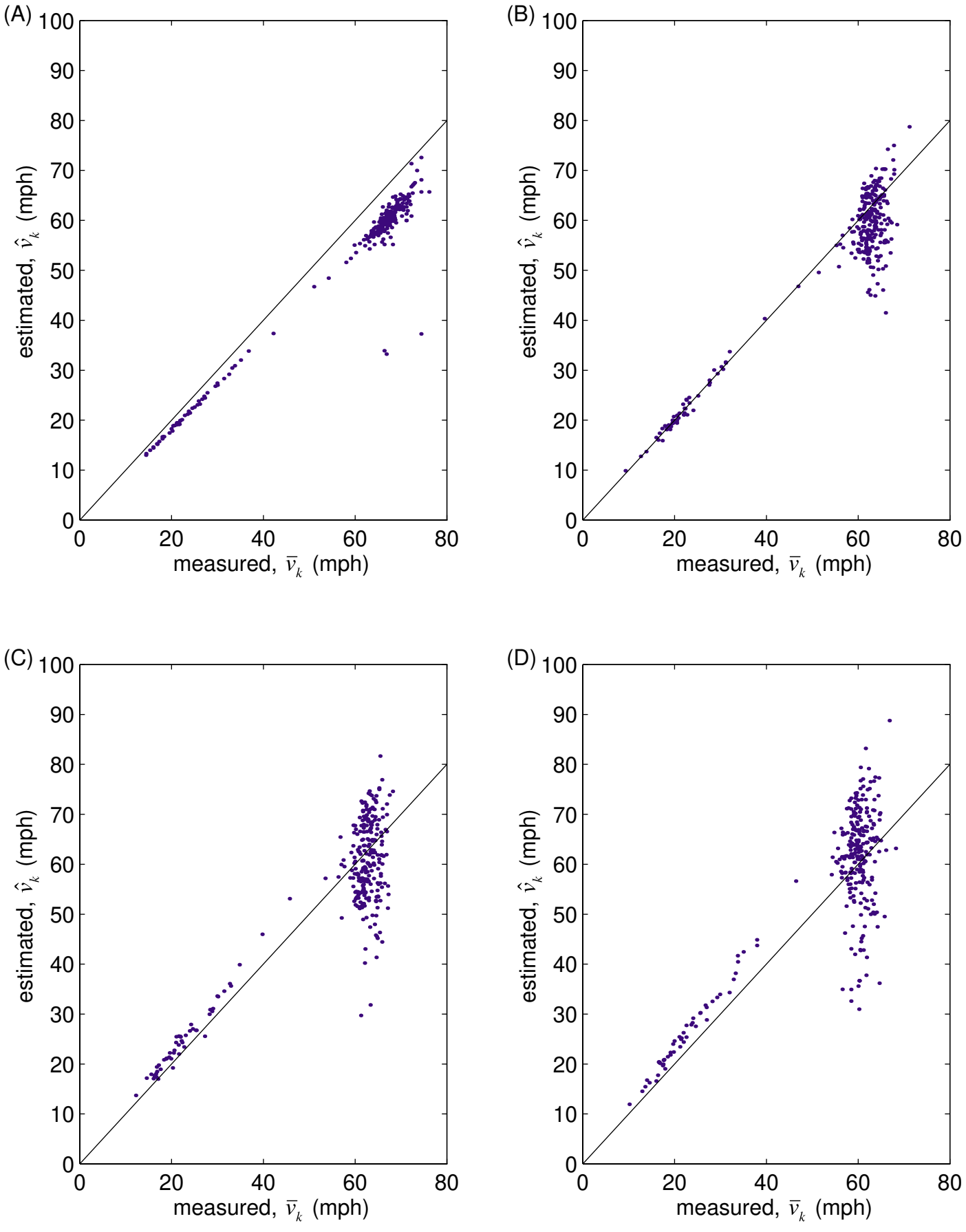

Figure 2-7, Contour plot showing the cumulative distribution of percent error in estimated velocity as a function of $\hat{L}$, (A)-(B) T = 30 sec, (C)-(D) T = 5 min, for (A) & (C) lane 1 eastbound, (B) & (D) lane 5 westbound.

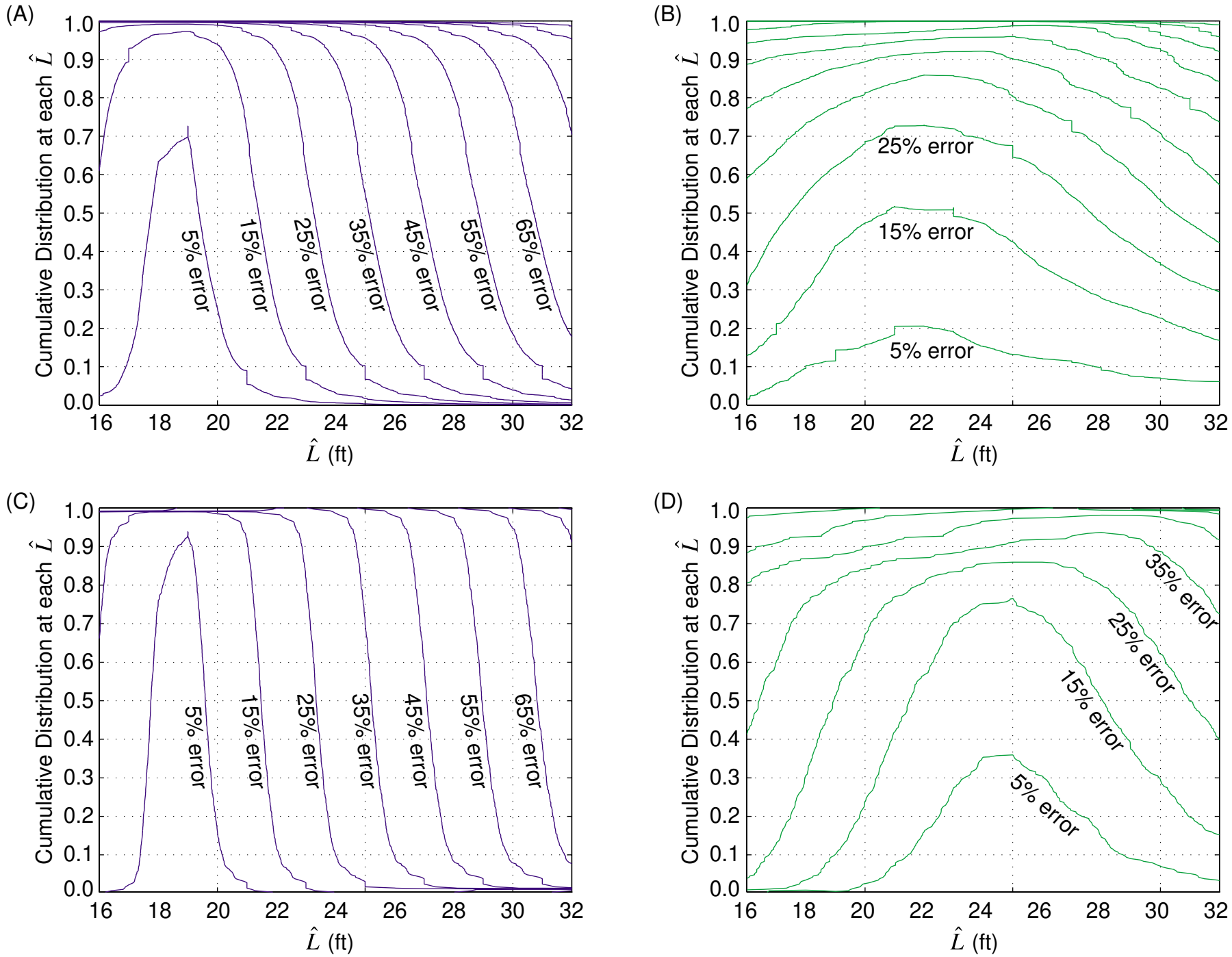

Figure 2-8, Estimated velocity after identifying low occupancy samples versus measured velocity, eastbound traffic, T = 5 min, (A) lane 1, (B) lane 2, (C) lane 3, (D) lane 4.

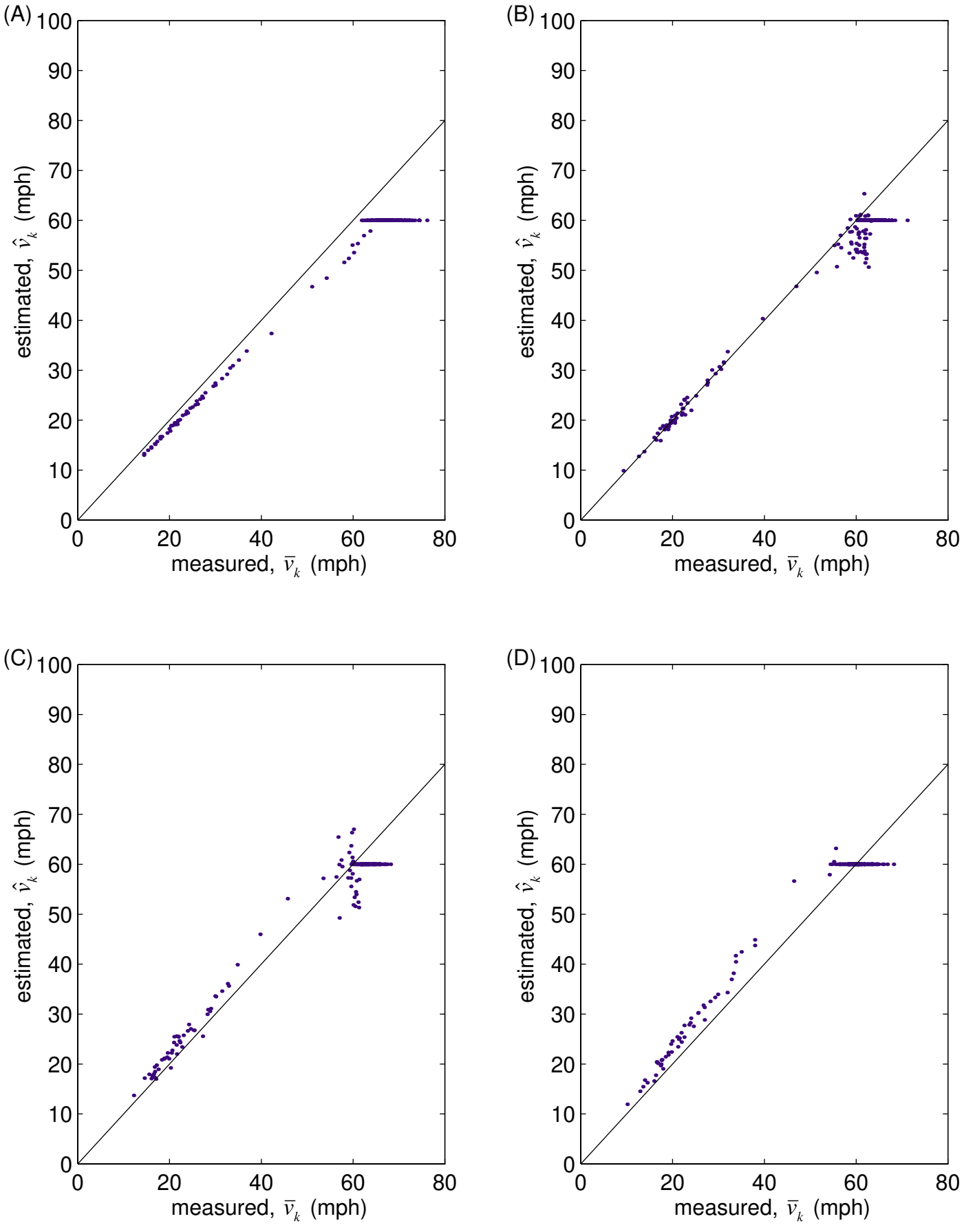

Figure 2-9, (A) Estimated velocity before identifying low occupancy samples, $\hat{v}_k$, eastbound traffic, T = 5 min and the corresponding (B) estimates after identifying low occupancy samples, (C) measured velocities, $\overline{v}_k$.

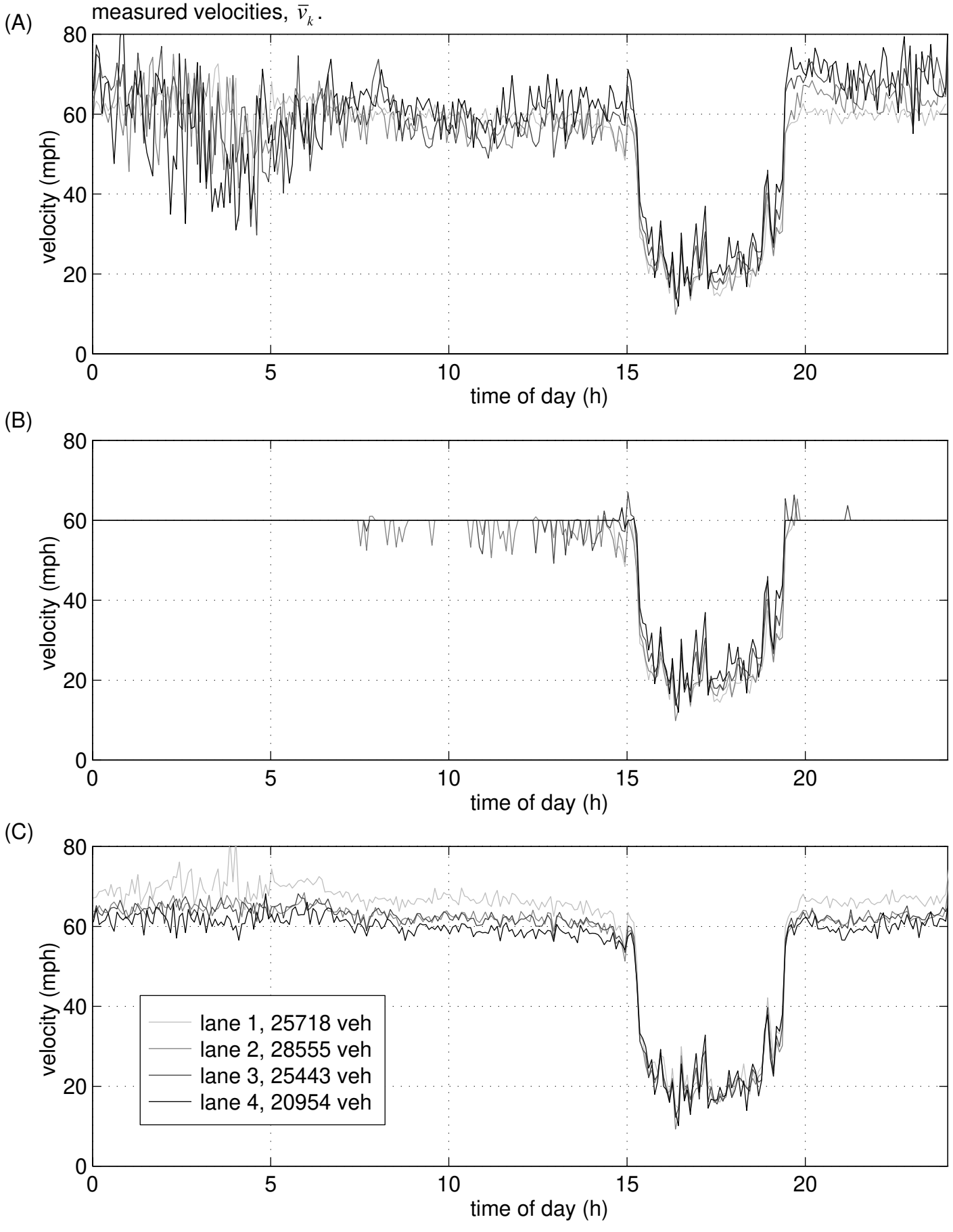

Figure 2-10, (A) Estimated velocity before identifying low occupancy samples, $\hat{v}_k$, westbound lane 3, T = 30 sec and the corresponding (B) estimates after identifying low occupancy samples, (C) measured velocities, $\overline{v}_k$.

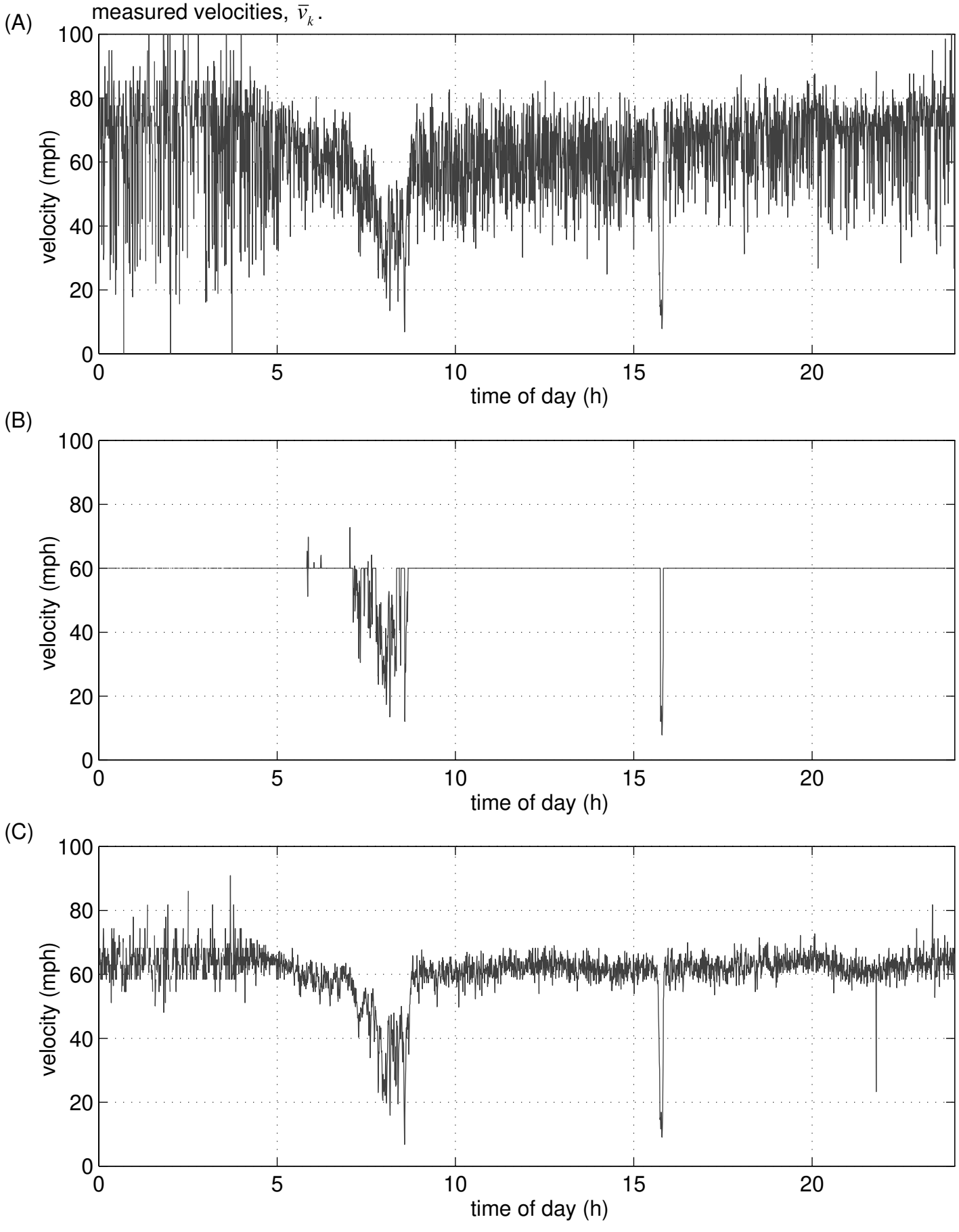

Figure 2-11, (A) The g-factor versus occupancy, T = 30 seconds, lane 1 eastbound, (B) with occupancy rounded down to integer values, (C) using time mean speed and rounded occupancy.

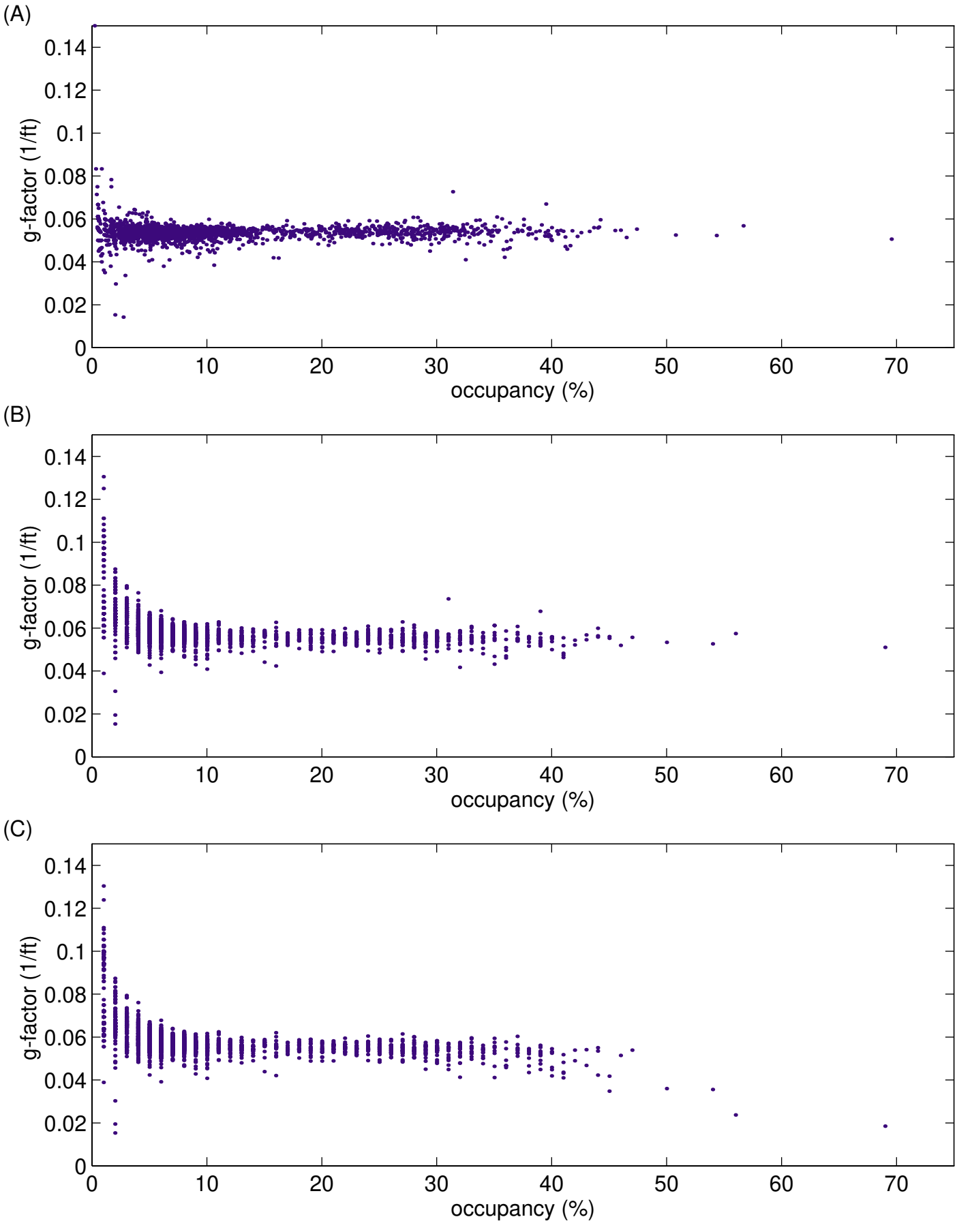

Figure 2-12, Mean g-factor calculated various ways versus occupancy, T = 30 seconds, for eastbound lane 1. (A) The aggregation method used by Hall and Persaud shown with "X"'s contrasted against the method advocated by this work, (B) the results from two additional aggregation methods.

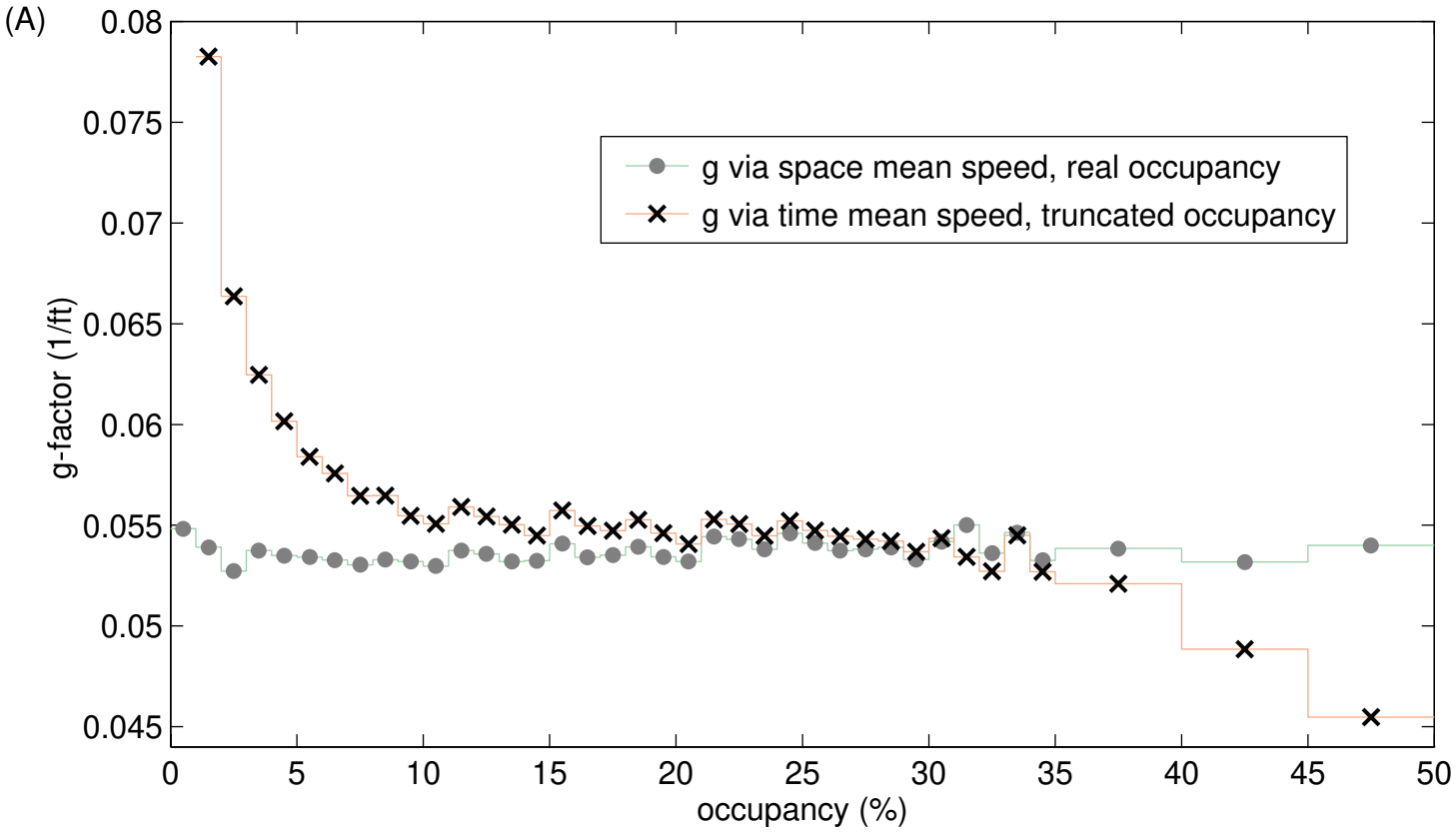

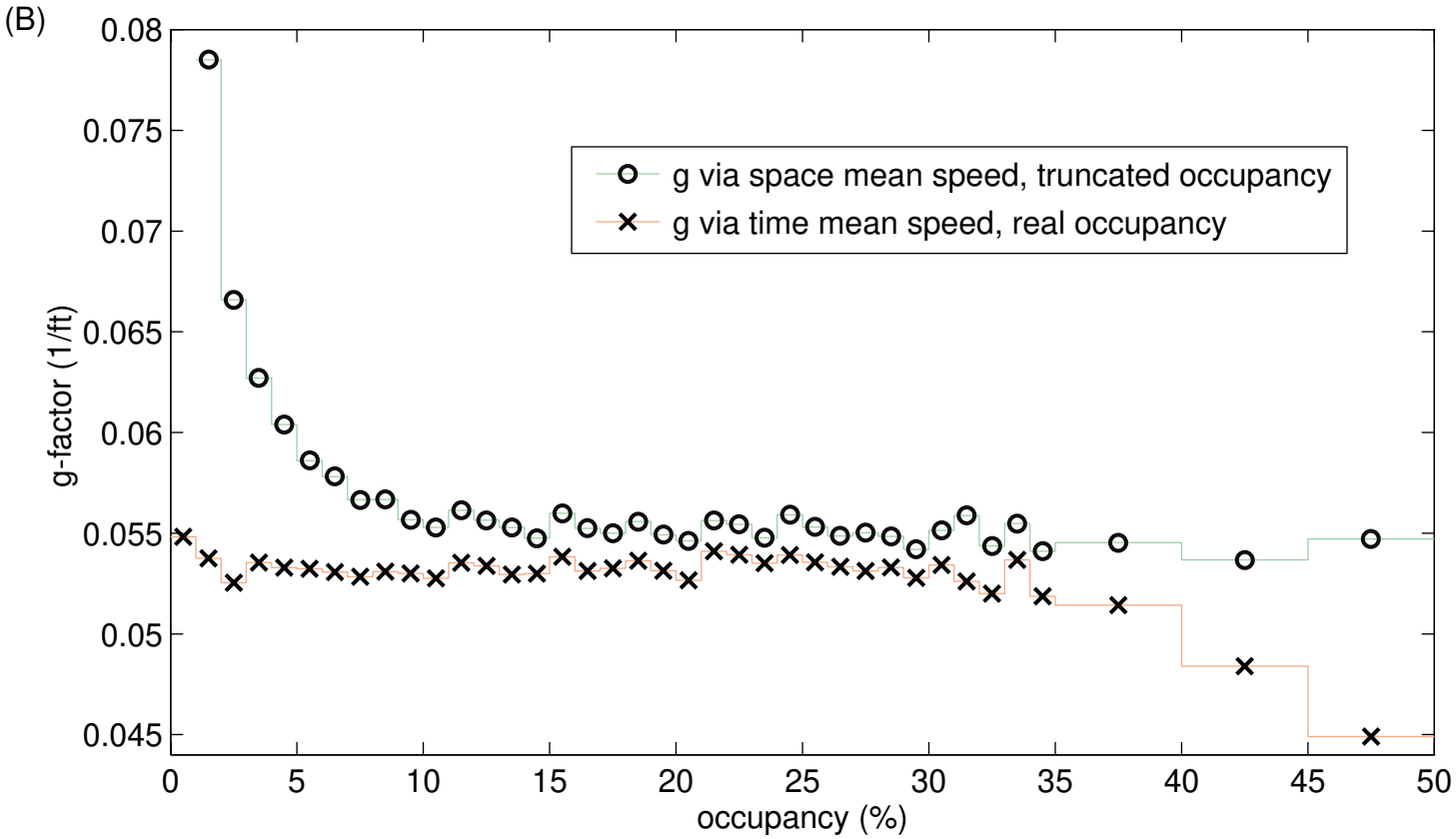

Table 2-1, The resulting estimates of $\hat{L}$ for the eastbound traffic

Lane	$\hat{L}$ (feet) T = 30 sec	$\hat{L}$ (feet) T = 5 min
1	16.8	16.9
2	19.6	19.9
3	21.3	22.0
4	21.8	22.8

3 ESTIMATING MEDIAN VELOCITY INSTEAD OF MEAN VELOCITY AT SINGLE LOOP DETECTORS

3.1 Introduction

Section 2 has shown a fundamental shortcoming with conventional estimates of velocity from single loop detectors. These estimates presume a "mean vehicle length"[2] that applies to all samples, but section 2 has shown that this assumption breaks down because a given sample may not be representative of the "average vehicle". In addition to loop detectors, there are many non-intrusive vehicle detectors that rely on the same principles.

As previously noted, many researchers have investigated techniques to reduce the influence of long vehicles, e.g., Mikhalkin et al. (1972), Pushkar et al. (1994), Dailey (1999), Wang and Nihan (2000) and section 2 above. All of these studies used aggregate flow (q) and occupancy (occ) to estimate mean velocity. Rather than manipulating aggregate data, this section examines new aggregation methods to reduce the estimation errors.

The first subsection reviews the state of the practice and the related shortcomings of conventional velocity estimation from single loop detectors. The second subsection proposes an alternative method for estimating velocity. The next subsection contrasts the new approach against conventional estimates. The final subsection shows how the new approach can be used to estimate individual vehicle lengths from single loop detectors.

[2] Throughout this document, "length" refers to the "effective vehicle length" as *seen* by the detectors.

3.2 Conventional Velocity Estimation

Provided that vehicle lengths and vehicle velocities are uncorrelated, as shown in section 2 and elsewhere, harmonic mean velocity (mean v) and arithmetic mean vehicle length (L) for a given sample are related by the following equation:

$$mean\ v \approx \frac{q \cdot L}{occ} \tag{3-1}$$

However, these two variables cannot be measured independently at a single loop. Typically, an operating agency will set L to a constant value and use Equation 3-1 to estimate velocity from single loop measurements. But this approach fails to account for the fact that the percentage of long vehicles may change during the day or the simple fact that a sample may not include "typical" vehicle lengths. Particularly during low flow, when the number of vehicles in a sample is small, a long vehicle can skew occupancy simply because it takes more time for that vehicle to pass the detector. For example, section 2 showed that approximately 85 percent of the individual vehicle lengths observed at one detector station were between 15 and 22 feet, but some vehicles were as long as 85 feet, or roughly four times the median length.

In accordance with the law of large numbers, the sample distribution should become more representative of the entire population as the sample size increases, which in turn, increases with flow. Figure 3-1 shows a detail from Figure 2-4 that illustrates this phenomena using two common sampling periods (T). In part A, T=30 sec and the maximum number of vehicles per sample is so small that the observations fall into distinct columns, i.e., the first column contains observations with only one vehicle, the second column contains observations with only two vehicles, and so on. Notice that for both values of T, the range of L is inversely proportional to q.

3.3 Alternative Parameters

For this study, we examine 24 hours of detector actuations, sampled at 60 Hz, from a dual loop detector station in the Berkeley Highway Laboratory (Coifman et al., 2000). In the dual loop configuration it is possible to measure true vehicle velocities from the quotient of the loop separation and the difference in a vehicle's arrival time at each loop. While an individual vehicle's length is simply the product of its measured velocity and *on time*, i.e., the amount of time that the vehicle occupies the detector. The subject detector station includes five lanes in each direction. In an attempt to capture the temporal changes in observed vehicle lengths, the data were arbitrarily subdivided into non-overlapping, three hour long segments by lane. The two distributions shown in Figure 3-2 represent the "best" distribution (lowest vehicle length variance, at 8.16 ft^2) and "worst" distribution (highest vehicle length variance, at 217 ft^2) observed across the 80 subsets. Removing the temporal component, consider a sample of N vehicles drawn at random from the "worst" distribution. Intuitively, the sample mean vehicle length is likely to be biased towards long vehicles because of the extended tail. The median vehicle length, however, should be less sensitive to the outliers. This hypothesis was verified using Monte Carlo simulation. The simulation consisted of 10,000 samples of N vehicles from each distribution, where N was set to 10, 50, 100, 500 and 1000 vehicles, and the sample mean and median were calculated. Table 3-1 summarizes the 99 percent confidence intervals for the mean and median lengths. The mean length confidence interval was significantly worse than the median length under all conditions. In fact, the results show that the range of the confidence interval for the median length of N vehicles is roughly proportional to that of the mean length for $10 \cdot N$ vehicles in this set. If we continue to assume that individual vehicle length and velocity are uncorrelated, then the simulation results lead to the following postulate:

$$median\ v \approx \frac{L}{median\ on\ time} \tag{3-2}$$

where the value of L may differ from that used in Equation 3-1.

3.4 Estimating Velocity

For both Equations 3-1 and 3-2, with a fixed L, one can consider the function on the right hand side as an estimate of the variable on the left hand side. Using the entire day's worth of data from each lane and setting the sample size to N consecutive vehicles in a given lane, Figures 3-3 and 3-4 show scatter plots of the estimates versus the corresponding measurements for two different values of N. In each figure, the left and right plots come from the same samples and L is assumed to be 20 feet in all plots. The choice of a different L would simply scale the estimates vertically, proportional to L/20. In both figures, the mean velocity estimate is much noisier than the median velocity estimate. Notice that the median velocity and its estimate tend to fall into discrete columns and rows, respectively, due to the resolution of the 60 Hz measurements. With N=10, the mean estimate is subject to errors from long vehicles throughout all traffic conditions, as highlighted with the circles in Figure 3-3. At larger N, Figure 3-4, the error is only evident during free flow conditions. This bias is due to the fact that trucks represent a larger percentage of the vehicle fleet in the early morning hours, a period when there was no observed congestion. To quantify these errors, we define the Measure of Variance (MOV) and Measure of Bias (MOB) over n samples as follows:

$$MOV = \frac{\sum_{i=1}^{n}\left(x_i^* - \hat{x}_i\right)^2}{n} \tag{3-3}$$

$$MOB = \frac{\sum_{i=1}^{n}\left(x_i^* - \hat{x}_i\right)}{n} \tag{3-4}$$

where x_i^* is the true value of the given variable for the i-th sample and $\hat{x}_i$ is the corresponding estimate. The resulting MOV and MOB for the velocity estimates from five different sample sizes are shown in the first few columns of Table 3-2. In each case, the MOV for the median velocity estimator is approximately one third of that for the mean velocity estimator. Of course,

the MOV is sensitive to the choice of L. So the analysis is repeated in the latter columns with L selected such that MOB=0 for the given sample size and estimator. This latter analysis reflects the performance when the unbiased L is used with the subject data set.

The estimates thus far are based on samples of a fixed number of vehicles. But the fixed number sampling is not very informative if the freeway is blocked or flow drops for some other reason. So in practice, it is better to sample over fixed time periods. Fixed time sampling has the added benefit that all samples can be synchronized at a detector station and thus, requires less computational and communications overhead. It is important, nonetheless, to ensure that the sample period is large enough to ensure a sufficient number of vehicles in a sample during any period when surveillance is desired. Looking at Figure 3-3 and Table 3-2, N=10 vehicles appears to provide satisfactory results for the median estimate, but this sample size is a little low for the mean estimate. With T=30 seconds, this criteria would require q>1200 veh/hr throughout the entire day. Applying this sampling period to the data results in very poor performance by both estimation techniques (see Table 3-2). On the other hand, if T=5 minutes, the criteria only requires q>120 veh/hr. Repeating the preceding analysis with T=5 minutes yields Figures 3-5 and 3-6. In Figure 3-5, one can see significant errors in the mean estimate and few errors in the median estimate. The corresponding statistics are reported in Table 3-2 and the performance appears to be on the order of fixed samples with N=10 vehicles for this data set. Figure 3-6 shows that the flow is quite low at this site for at least four hours in the early morning and it is above 1200 veh/hr for only about half of the day. The reader should also note that this location sees a relatively large volume of traffic, with an average of approximately 25,000 vehicles/lane/day. Most other locations will have a lower average daily flow, reaffirming the need for longer sample periods.

Although T=5 minutes appears to provide sufficient sample size, the long delay between measurement updates may be undesirable. Fortunately, many applications only need a single

estimate of velocity for a given detector station or link. To keep N high while reducing T, one can sample across multiple lanes before estimating velocity. In particular, setting T=30 seconds and sampling individual vehicle measurements across the four outside lanes in a given direction yields Figure 3-7 and the final row of statistics in Table 3-2. Note that the inside lane was excluded because it is a high occupancy vehicle (HOV) lane in both directions

Finally, one could extend this work to design a hybrid sampling criteria for each lane, one that only uses the N most recent vehicles provided they pass during the preceding T time period. If this criterion is not met, only use those vehicles that pass during the time period. The reporting rate can be faster than T, e.g., N=10, T=5min and report the most recent observations every 30 sec.

3.4.1 Discussion

The various sampling criteria were used to illustrate the fact that Equation 3-2 performs better than conventional estimates from Equation 3-1 no matter how the vehicles are sampled. It is worth noting that Courage et al. (1976) used simulation to conduct a detailed analysis of conventional velocity estimates under various sampling criteria. In the present study, L = 20 ft and T = 5 min give satisfactory results. Of course the required accuracy and sampling period depend on the application. Due to the limited number of detector stations that provide individual vehicle data, the authors have not been able to apply the work to other locations. An operating agency interested in experimenting with this methodology might want to start with these settings, examine the resulting estimates over several days and then adjust as needed.

Figure 3-8A compares the true median velocity to space mean speed in a typical lane using five minute samples, while Figure 3-8B compares the corresponding estimates. Obviously the median velocity and space mean speed differ slightly for most samples. Although there is no direct relationship between the two metrics, they are both measures for the *center* of the sample.

In contrast to conventional practice, the new estimate significantly reduces the velocity estimation errors when it is not possible to control for a wide range of vehicle lengths. Repeating the preceding analysis using Equation 3-2 as an estimate of space mean speed, rather than median velocity, yields Table 3-3. Except for N≥500, Tables 3-2 and 3-3 clearly show that the MOV from Equation 3-1 is larger than the MOV from Equation 3-2 when both methods are used to estimate space mean speed. The increasing MOV at large N in Table 3-3 should not be surprising. As the sample size increases, it is more likely that the prevailing velocity will change significantly during the observation period, thus, allowing for a greater difference between the true mean and median velocities.

Of course the use of Equation 3-1 is based on the assumption that individual vehicle velocities and lengths are uncorrelated. In the event that vehicle length and velocity are inversely proportional, as is frequently the case in free flow traffic, a long vehicle will spend more time over the detector and the associated *on time* will be larger. This increase will impact the occupancy measurement (which is proportional to the mean *on time*) more than the median *on time*. Thus, the performance of Equation 3-1 would be expected to degrade worse than the performance of Equation 3-2 under these conditions.

Of course the median estimates might degrade in the presence of high truck volumes. To address this fact, Equation 3-2 could be modified to select a different percentile from the observed distribution of *on times*, e.g., the 25th percentile rather than the median. Additional information could also be used, such as the presence of truck restrictions in specific lanes or slightly more complicated models that exclude low flow conditions, e.g., section 2. Finally, note that heavy truck flows would likely have a greater impact on the conventional estimates from Equation 1.

3.5 Estimating Vehicle Lengths

Assuming the loop detector is functioning properly, a given measured *on time* is simply a function of the vehicle's length and velocity. During free flow conditions the vehicle velocities

typically fall in a small range and during congested conditions the difference between successive vehicles' velocities is usually small. If one assumes that all of the vehicles in a sample are traveling near the median velocity, one can use Equation 3-2 in conjunction with measured *on times* to estimate individual vehicle lengths with the following equation,

$$\hat{l}_j = \hat{v}_i \cdot on_j \tag{3-5}$$

where

$\hat{l}_j$ = estimated vehicle length for the j-th vehicle in the i-th sample

$\hat{v}_i$ = estimated median velocity for the i-th sample

on_j = measured *on time* for the j-th vehicle in the i-th sample.

Of course the number of vehicles per sample must be small enough for the velocity assumption to hold and one must control for low velocity conditions, when acceleration becomes non-negligible during the sample. Using N=10 and restricting the analysis to all samples with $\hat{v}_i$>20 mph, the average error in $\hat{l}_j$ is less than six percent for the 210,000 vehicles in the data set that satisfy the velocity constraint. The length estimates can be improved further by calculating the median velocity for the N vehicles centered on the subject vehicle, but this approach requires the observation of subsequent vehicles and it is more computationally intensive.

3.6 Conclusions

Many researchers have sought better estimates of velocity from single loop detectors. The earlier works have emphasized techniques to reduce the bias from long vehicles in mean velocity estimates. This section has taken a different approach, it uses a new aggregation methodology to estimate median velocity and it was shown that the estimate is less sensitive to the presence of long vehicles. This fact leads to the added benefit that the assumed value of L is less sensitive to site-specific characteristics of the traffic flow. As shown in Tables 3-2 and 3-3, the new

methodology significantly reduces velocity estimation errors at single loop detectors when it is not possible to control for a wide range of vehicle lengths.

It may seem intuitive that the median is less sensitive to outliers than the mean, but it does not appear that this fact has previously been employed for estimating velocity from single loops. Although the median is less sensitive to outliers, it is still necessary to observe several vehicles in a given sample to reduce the impact of long vehicles and it is not advisable to estimate velocity with short sample periods during low flow conditions. To this end, two methods for increasing N while keeping T low were proposed. The first approach combined data from multiple lanes before estimating velocity and yielded satisfactory results on the experimental data set. The second approach would use a hybrid sampling criteria to switch between fixed number of vehicles and fixed time sampling. Finally, the discussion anticipated potential problems with heavy truck flows and suggested several possible solutions to reduce these impacts.

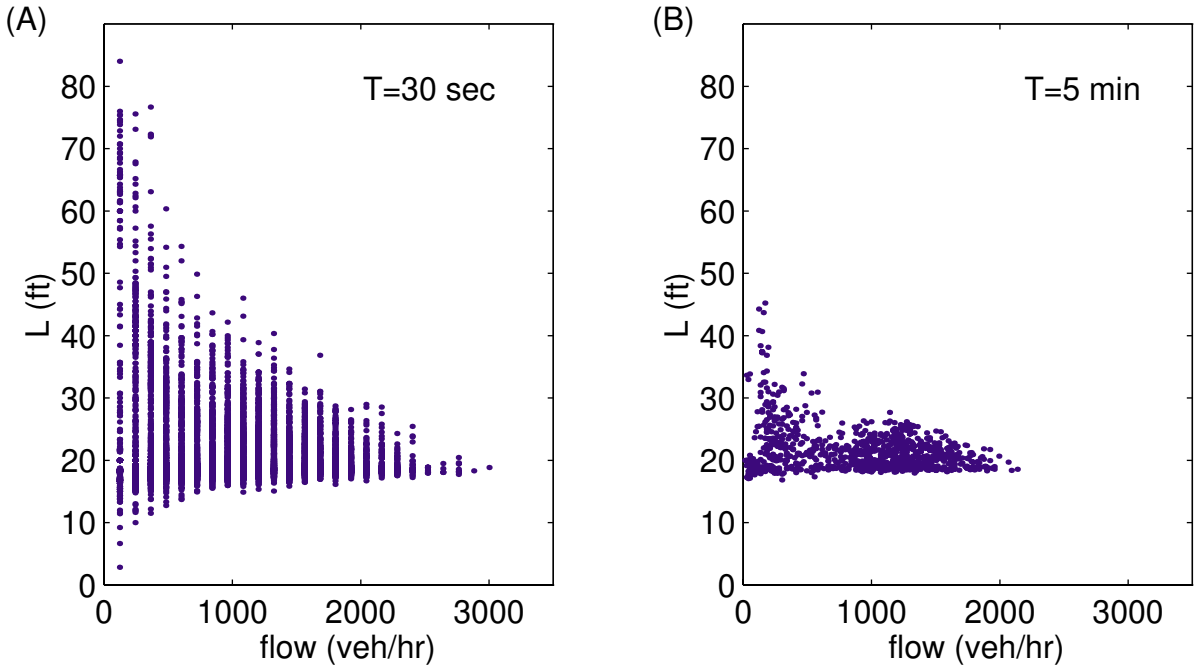

Figure 3-1, Observed average effective length versus flow for five lanes at one detector station, over one day, sampled at (A) T = 30 sec, (B) T = 5 min.

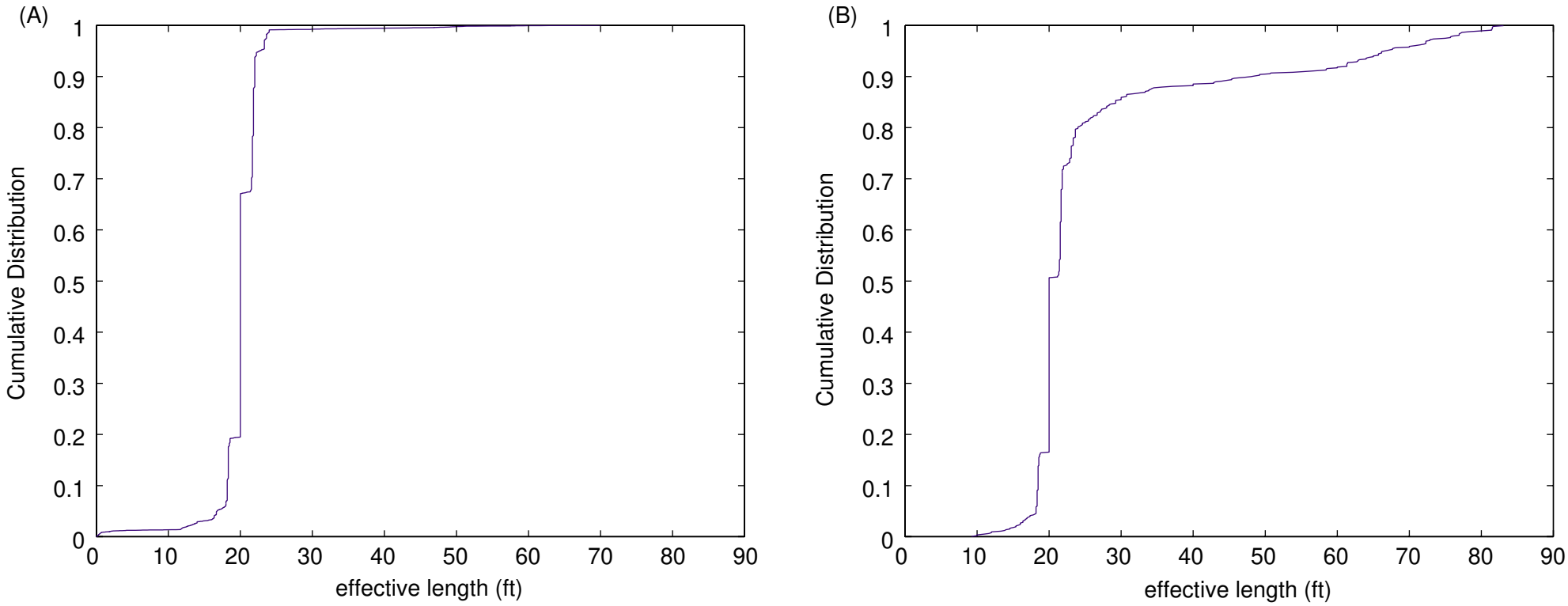

Figure 3-2, Observed distributions of individual effective vehicle lengths in a single lane for three hour periods. (A) lowest variance or "best" case, (B) highest variance or "worst" case.

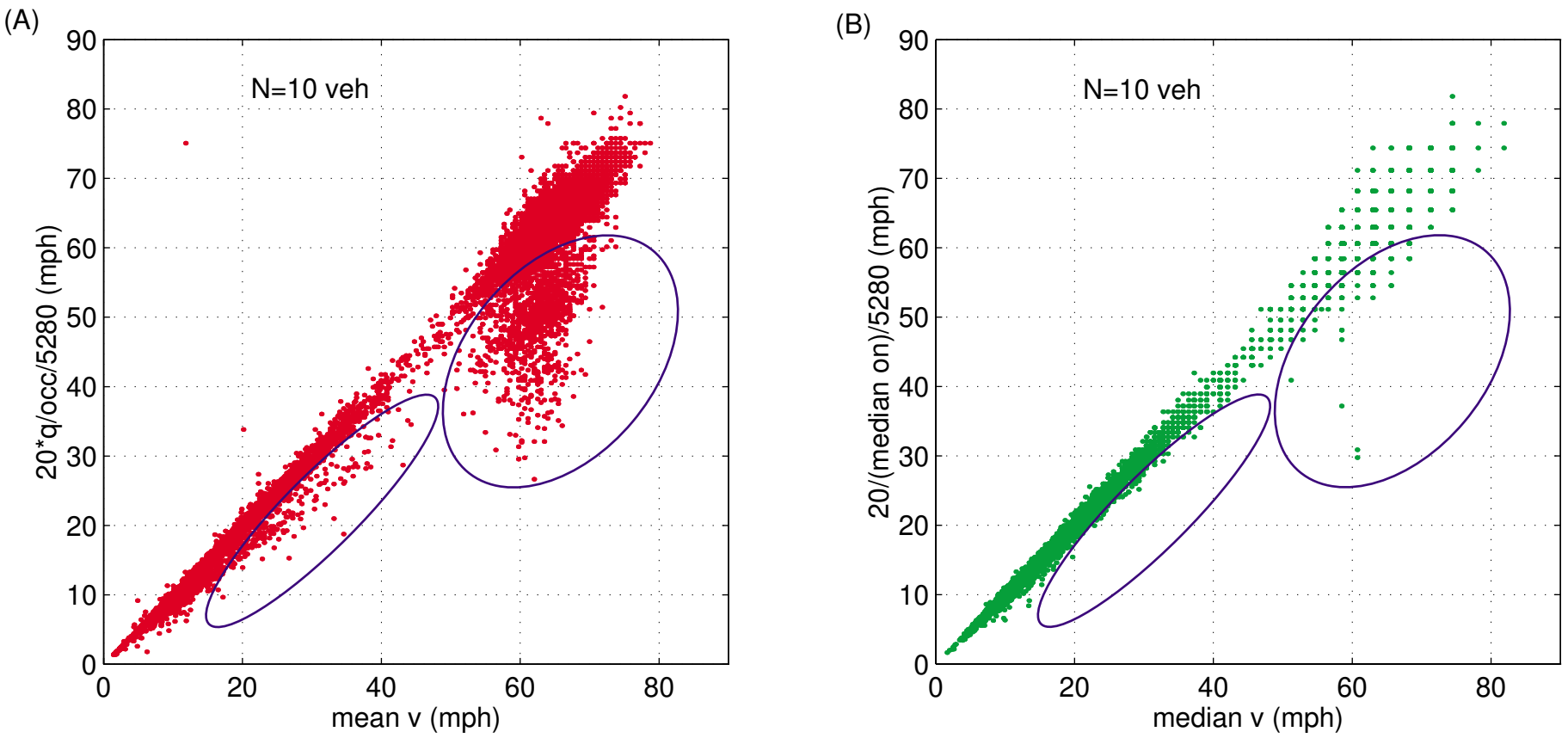

Figure 3-3, This figure uses real traffic data to compare estimated versus measured (A) mean velocity (B) median velocity for 24,640 samples of 10 vehicles each. Note that the circles were added to the same locations in both plots to highlight the differences.

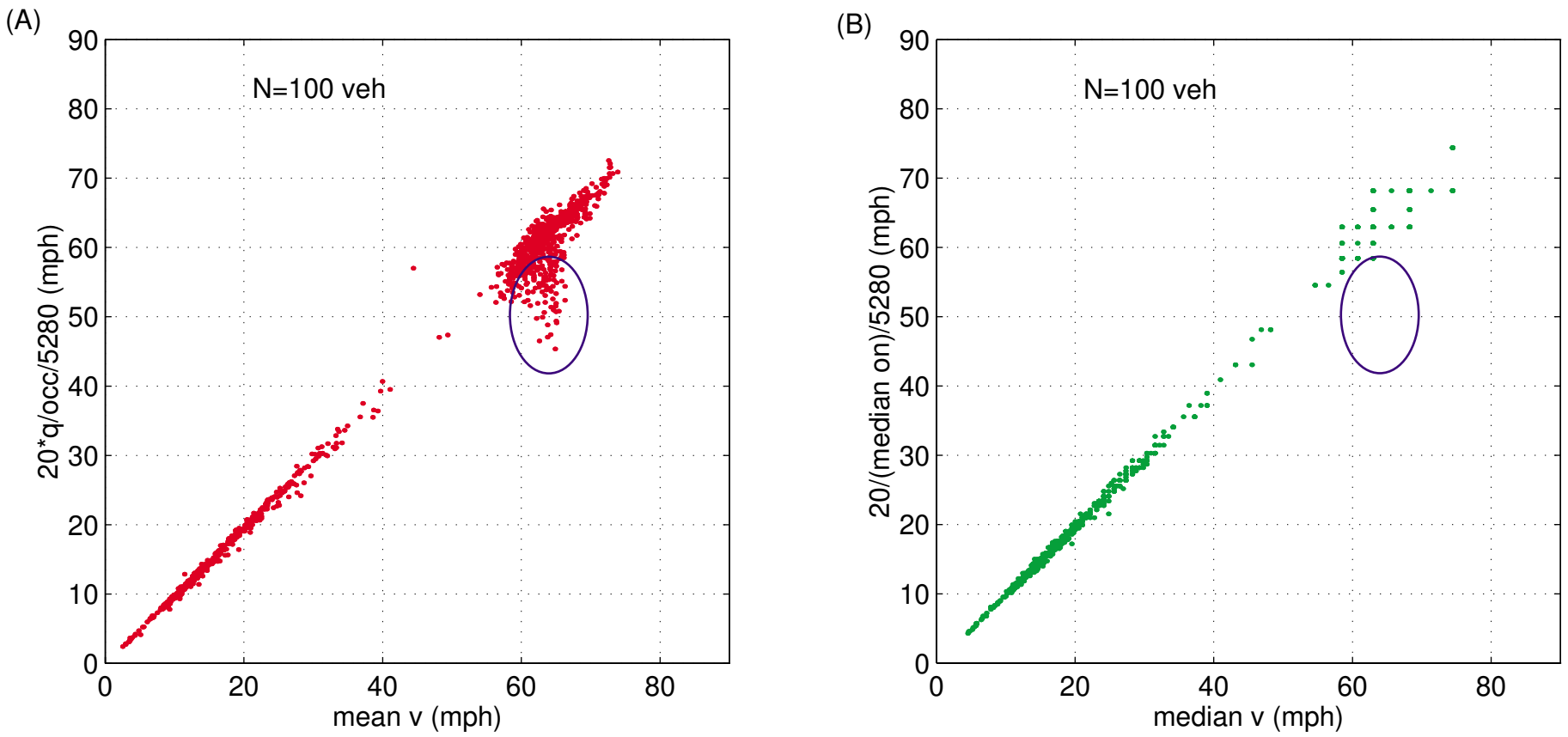

Figure 3-4, Now using samples of 100 vehicles each, this figure compares estimated versus measured (A) mean velocity (B) median velocity for 2,460 samples. Again, the circles were added to the same locations in both plots to highlight the differences.

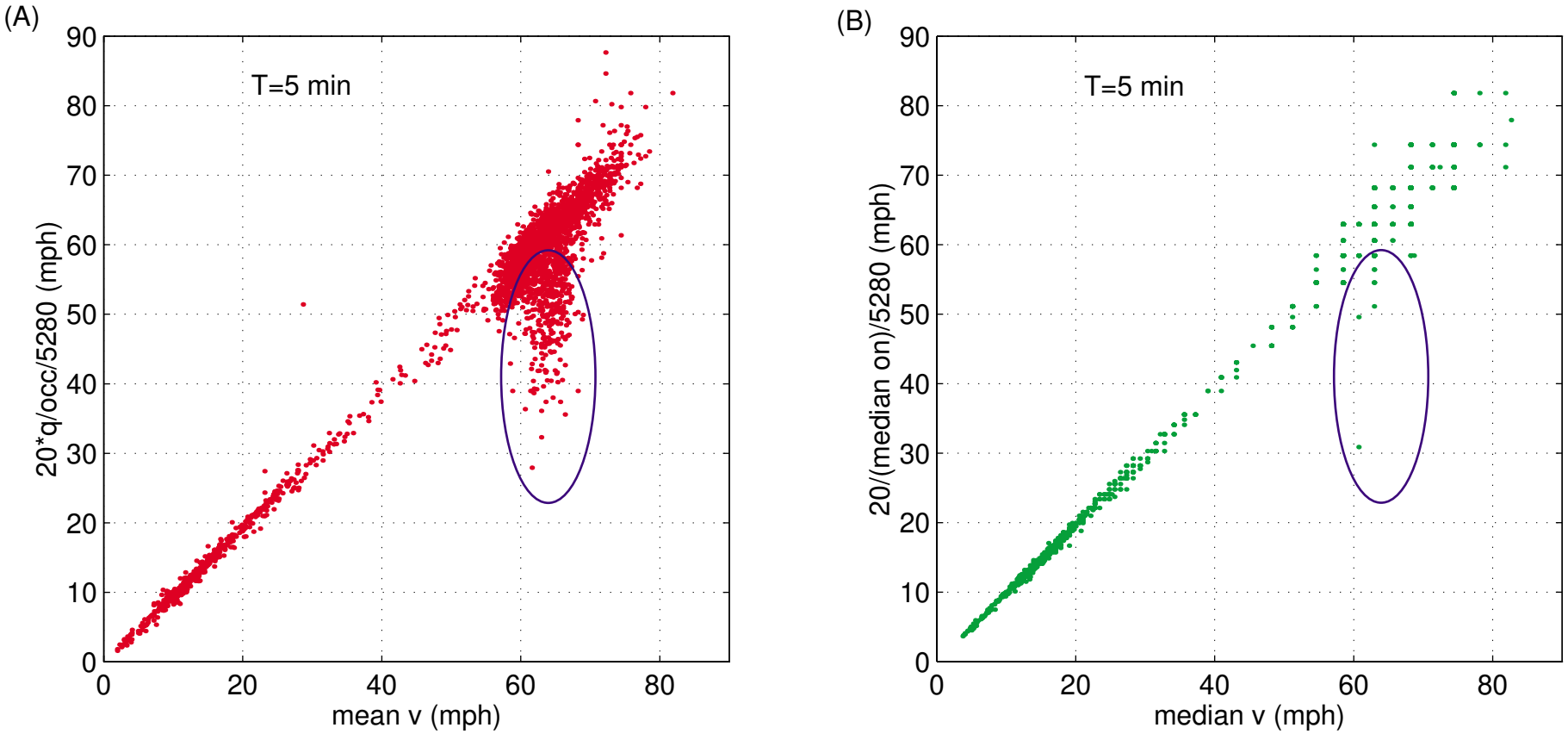

Figure 3-5, Moving to a fixed sample period of 5 minutes, this figure compares estimated versus measured (A) mean velocity (B) median velocity for 2,870 samples. Again, the circles were added to the same locations in each plot to highlight differences.

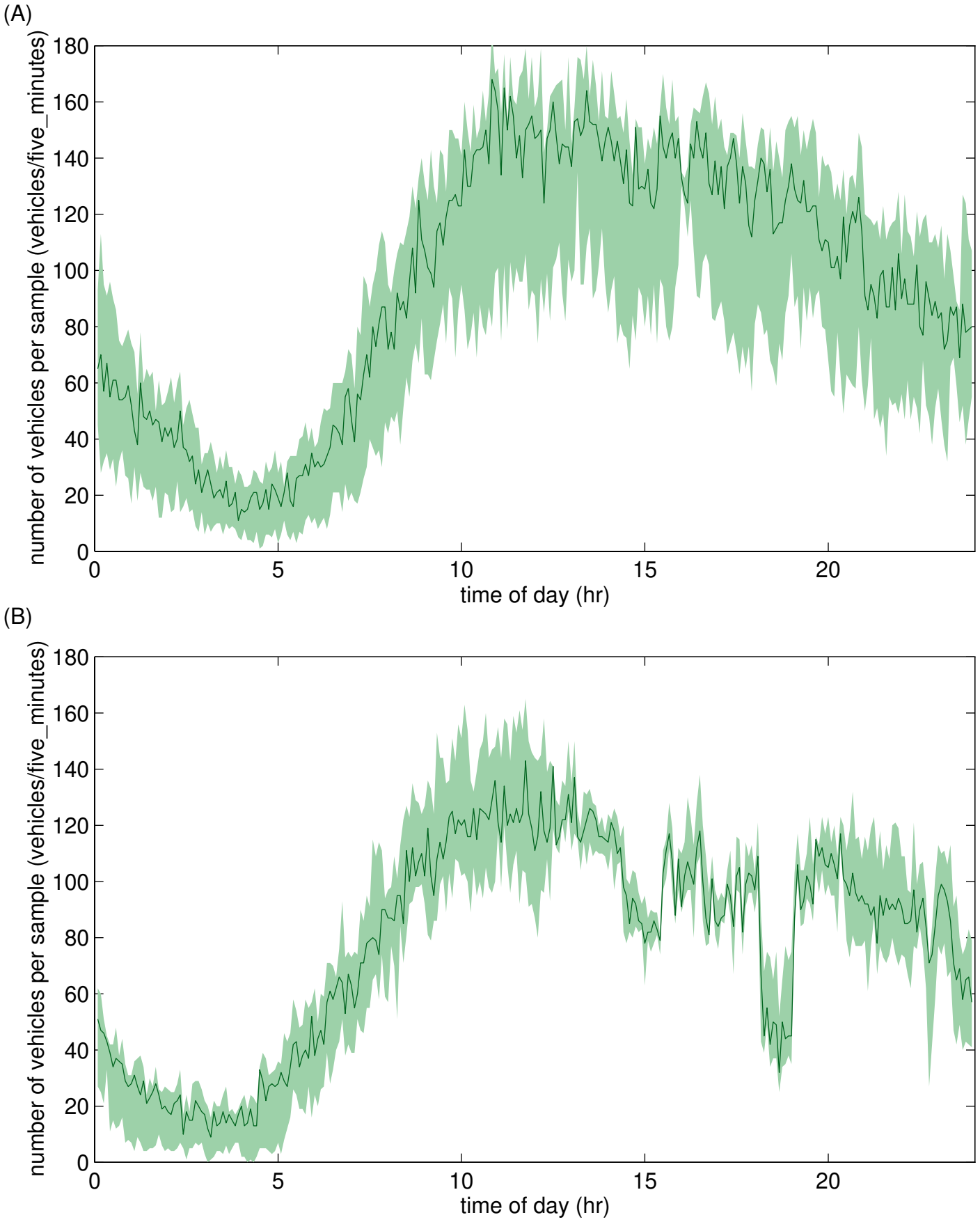

Figure 3-6, Range of observed sample sizes (light region) and median sample size (solid line) across five adjacent lanes for the data shown in the previous figure (A) northbound lanes, (B) southbound lanes.

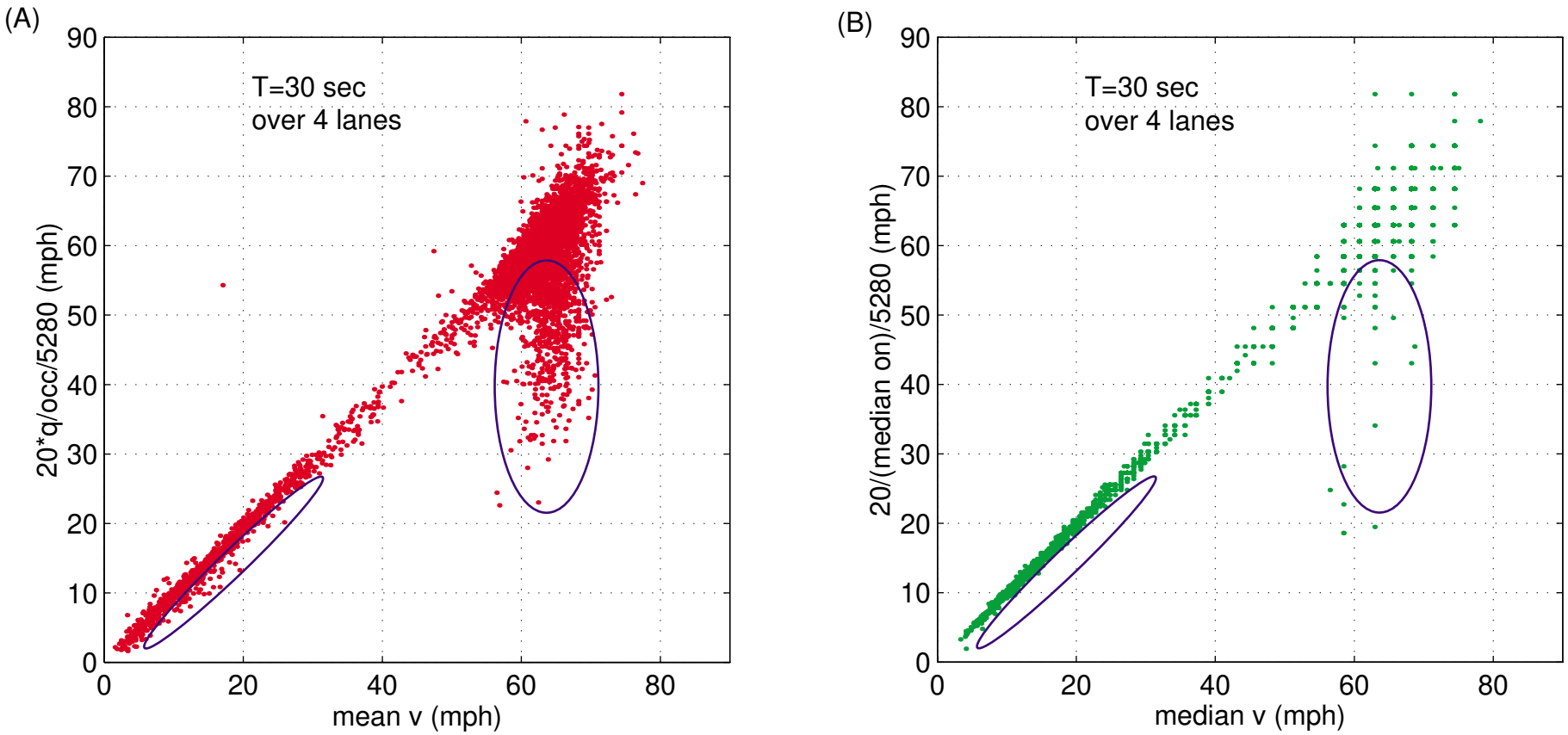

Figure 3-7, Finally, using a fixed sample period of 30 seconds and combining data over four lanes, this figure shows estimated versus measured (A) mean velocity (B) median velocity for 5,760 samples. Once more, the circles highlight the differences between the plots.

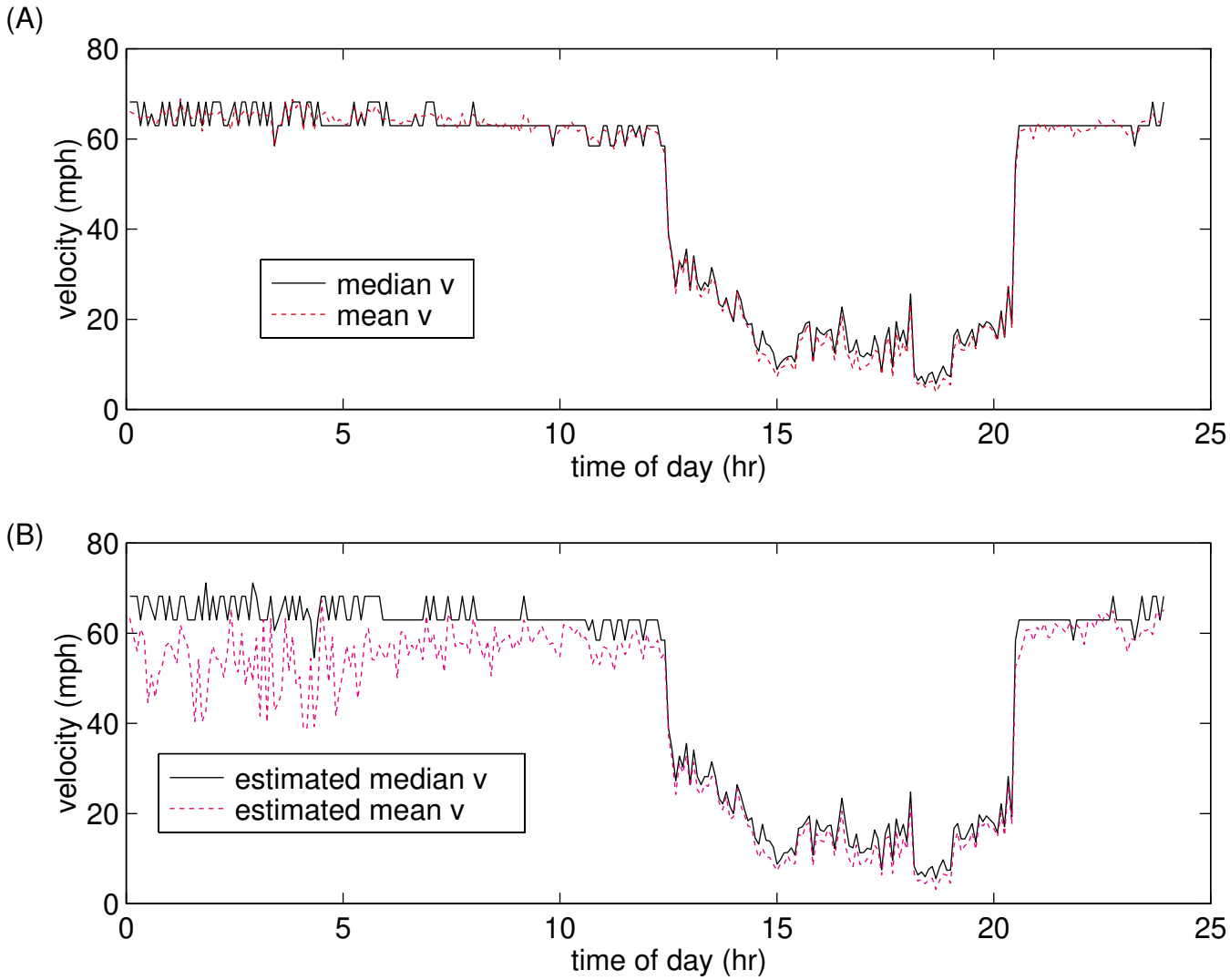

Figure 3-8, (A) Observed mean and median velocity for five minute samples in a single lane. (B) Corresponding estimates from Equations 1 and 2.

Table 3-1, Confidence intervals for mean and median effective vehicle length from Monte Carlo simulation for various sample sizes from the "best" and "worst" observed distributions.

		99 percent confidence intervals of vehicle length (ft)					
		for mean			for median		
		upper bound	lower bound	difference	upper bound	lower bound	difference
from "best" distribution	N=10 veh	25.07	16.65	8.42	21.82	18.45	3.37
	N=50 veh	21.78	18.75	3.03	20.77	20.00	0.77
	N=100 veh	21.27	19.16	2.11	20.00	20.00	0.00
	N=500 veh	20.59	19.71	0.88	20.00	20.00	0.00
	N=1000 veh	20.45	19.82	0.63	20.00	20.00	0.00
from "worst" distribution	N=10 veh	40.77	19.03	21.74	27.69	19.23	8.46
	N=50 veh	32.07	21.42	10.65	21.74	20.00	1.74
	N=100 veh	30.23	22.62	7.61	21.67	20.00	1.67
	N=500 veh	27.89	24.42	3.47	21.54	20.00	1.54
	N=1000 veh	27.34	24.88	2.46	21.45	20.00	1.45

Table 3-2, Measure of Variance (MOV) and Measure of Bias (MOB) for estimated mean and median velocity using different sampling criteria on the same set of vehicle measurements. Note that these data come from real observations rather than simulation.

		L set to 20 feet				L set to eliminate bias			
		MOV $(mph)^2$		MOB (mph)		MOV $(mph)^2$		L (ft)	
sampling criteria	number of samples	for mean v	for median v	for mean v	for median v	for mean v	for median v	for mean v	for median v
N=10 veh	24640	26.63	7.22	2.44	1.03	21.62	6.15	20.96	20.39
N=50 veh	4920	17.10	5.58	2.71	1.09	9.36	4.28	21.08	20.42
N=100 veh	2460	15.48	5.38	2.74	1.11	7.31	4.04	21.09	20.42
N=500 veh	490	13.99	4.92	2.77	1.00	5.37	3.84	21.12	20.38
N=1000 veh	235	13.54	5.09	2.78	1.05	4.77	3.86	21.13	20.40
T=30 sec	28750	63.69	29.23	2.82	1.35	60.94	28.48	21.08	20.50
T=5 min	2870	34.36	7.02	3.59	1.03	22.37	5.96	21.39	20.38
T=30 sec and combining 4 lanes	5760	47.39	8.73	4.02	0.98	33.12	7.85	21.59	20.36

Table 3-3, Measure of Variance (MOV) and Measure of Bias (MOB) when using Equation 2 as an estimate of space mean speed.

sampling criteria	L set to 20 feet		L set to eliminate bias	
	MOV $(mph)^2$	MOB (mph)	MOV $(mph)^2$	L (ft)
N=10 veh	6.99	0.88	6.02	20.34
N=50 veh	5.37	0.58	4.68	20.22
N=100 veh	5.22	0.43	4.73	20.16
N=500 veh	6.47	0.06	6.43	20.02
N=1000 veh	10.87	-0.34	11.04	19.87
T=30 sec	28.68	1.18	27.97	20.44
T=5 min	6.52	0.42	6.12	20.15
T=30 sec and combining 4 lanes	8.19	0.50	7.80	20.19

4 ESTIMATING TRAVEL TIMES AND VEHICLE TRAJECTORIES ON FREEWAYS USING DUAL LOOP DETECTORS

4.1 Introduction

A recent report from Caltrans noted that, "rapid changes in link travel time represent perhaps the most robust and deterministic indicator of an incident [and] link travel time ... is perhaps the most important parameter for ATIS functions such as congestion routing." (Palen, 1997) Similar views have lead the Federal Highway Administration and several states to develop and deploy new detector technologies capable of collecting true travel time data over extended freeway links, e.g., Balke et al., 1995, Coifman, 1998, Huang and Russell, 1997, Sun et al., 1999.

The emphasis on new technology to measure travel time is partially due to a misunderstanding of how to interpret vehicle travel times. For example, Sun et al. used conventional average velocity sampled at a detector station over fixed time periods as a base case in their analysis. The authors found that link travel times differed significantly from the quotient of local velocity and the link distance. But this result is not surprising, since the link travel time for a vehicle reflects traffic conditions averaged over a fixed distance and a variable amount of time, while the detector data only reflects traffic conditions averaged over a fixed time period at a single point in space.

In contrast to the naive approach of generalizing point measurements over an entire link, this section will show that judicious application of traffic flow theory can yield accurate link travel time estimates from point data. In particular, Lighthill and Whitham (1955) postulated that signals propagate through the traffic stream in a predictable manner and that a single curve in the flow versus density plane defines the set of stationary traffic states. When the state transitions from one point on the curve to another, the resulting signal should propagate through the traffic stream at a velocity equal to the slope of the line between the two points. Building off of this earlier work, Newell (1993) proposed a simplified flow density relationship, as shown in Figure

4-1. Provided the traffic state remains on one leg of the *triangle*, all signals should propagate at the same velocity: u_F for free flow or u_C for congested conditions. Windover and Cassidy (2000) have verified empirically that this simplification is reasonably accurate. If a freeway link does not contain a source of delay, such as a recurring bottleneck or an incident, then all of the signals that influence a vehicle's travel time must pass at least one end of the link at a known velocity.

If we postulate that traffic velocity, v, over time, t, and space, x, has the functional form

$$v(x,t) = f(x + u \cdot t) \tag{4-1}$$

where u is either u_F or u_C. Then, the level sets of function f are straight lines and thus, v is completely determined by observing this parameter over time at a single point in space, i.e., at a detector station. The evolution of vehicle trajectories in the time-space plane are defined by the differential equation

$$\frac{dx}{dt} = v(x,t) \tag{4-2}$$

and vehicle's link travel time is simply the time it takes the corresponding trajectory to propagate across the link, i.e., from one detector station to the next.

Using this postulate, the remainder of this section develops a methodology to estimate link travel times by integrating the signals that pass a dual loop detector, without deploying new hardware or combining data from multiple locations. The estimation method should be beneficial for traveler information applications, where travel time is considered more informative to users than average velocity. One could also view the estimation method as providing "expected travel times" without an incident. Used in conjunction with one of the new technologies capable of measuring the true vehicle travel times, a significant deviation between the expected and measured travel times would be indicative of congestion. Then, historical trends could be used to differentiate between recurring congestion and an incident. If a travel time estimation system

is deployed for real time traffic control, the system could also prove beneficial for planning applications such as quantifying congestion or model calibration. This last point is an important task for the traditional four-step planning process as well as the on-going Travel Model Improvement Program, which seeks to replace the process with microsimulation models. For example, the TRANSIMS designers at Los Alamos National Labs note that "The most important result of a transportation microsimulation in [the planning] context should be the delays..." (Nagel et al., 1998). Finally, in the process of developing the estimation method, this section will also show how it can be used to estimate vehicle trajectories over a freeway link, which in turn could be useful for quantifying vehicle emissions and other applications.

4.2 Travel time estimation

A dual loop detector station is capable of recording vehicle velocities and arrival times at a single point in space. We use this information to define a *chord* in the time-space plane, where a chord is simply a straight line with a slope equal to a vehicle's measured velocity and passes the location of the detector at the instant the vehicle passes. Figure 4-2A shows a single chord for a detector at zero distance and Figure 4-2B adds the next 13 chords recorded at the detector. Empirically, the chords provide a rough approximation of vehicle trajectories for a short distance downstream of the detector, but the approximation quickly breaks down, as evidenced by the intersection of several cords in Figure 4-2B. Assuming that individual vehicle measurements represent discrete observations from a slowly varying traffic state at the detector location, the changing state can be approximated by discrete samples equal to the vehicle headways. During congested conditions, i.e., the right hand leg of the curve in Figure 4-1, the transition between one discrete state and another should propagate at u_C. In other words, a vehicle passage represents an observed signal. These signals are shown with dashed lines in Figure 4-2C, where each chord is truncated as soon as it reaches the next observed signal. Figure 4-3 shows the

relationships between u_C, vehicle velocity, v_j, headway, h_j, travel time, τ_j, and distance traveled, x_j, for j-th truncated chord. It is a simple exercise to show that,

$$\tau_j = \frac{h_j}{1 + v_j / u_C} \tag{4-3}$$

$$x_j = v_j \cdot \tau_j \tag{4-4}$$

Because all signals are assumed to travel at the same speed, the parameters from Figure 4-3 are the same for any vehicle passing through a given *band* between two signals. Connecting the truncated cords end-to-end yields an estimated trajectory, shown in Figure 4-2D, for the vehicle from part A. In practice, one need only add up successive x_j's until the total exceeds the link distance. The sum of the corresponding τ_j's yields a travel time estimate. To enumerate the steps in this estimation, first, measure h_j and v_j then calculate x_j and τ_j using Equations 4-3 and 4-4. For the k-th vehicle, find the largest N_k such that,

$$d \geq \sum_{j=k}^{k+N_k} x_j \tag{4-5}$$

where d is the length of the link and N_k+1 represents an estimate of the number of vehicles that pass the detector while the k-th vehicle traverses the link. Typically the link distance will exceed the sum of x_j's by some percentage of the next x_j, so a better estimate of travel time will include the corresponding τ_j, weighted by the same percentage. More formally, calculate a weight, p, as follows,

$$p = \frac{\left(x_{k+N_k+1} + \sum_{j=k}^{k+N_k} x_j \right) - d}{x_{k+N_k+1}} \tag{4-6}$$

Finally, calculate the estimated travel time, T_k,

$$T_k = p \cdot \tau_{k+N_k+1} + \sum_{j=k}^{k+N_k} \tau_j \qquad (4\text{-}7)$$

Another improvement comes by recognizing that h_j occurs between vehicle observations. So the harmonic mean of two successive velocity measurements, v_j and v_{j+1}, should be more representative of conditions during the j-th band than either velocity measurement taken alone. The remainder of this section uses this improvement. It is a simple extension to show that rotating Figures 4-2 and 4-3 by 180 degrees, the methodology can also be applied to traffic upstream of a detector. Lastly, to estimate the k-th vehicle trajectory, one only need calculate the cumulative sum at each j from Equations 4-5 and 4-7.

4.2.1 A Short Example

This example applies the travel time estimation methodology during congested conditions, over an 1,800 foot long freeway link that does not contain any ramps. Dual loop detector stations bound the link on either end (see Coifman et al., 2000 for more information). In this configuration, each detector station can be used to generate an independent estimate of travel time over the link. Before making this estimate, one must settle on a value of u_C. Examining a different freeway, Windover, 1998 found u_C had a small variance from signal to signal and most signals during congested conditions traveled between 12 mph and 16 mph. The velocity range was manually verified at the subject link by comparing extrema points in time series flow and occupancy at either end of the link. A constant value of 14 mph is assumed for u_C throughout the rest of the section.

Examining a single lane, the solid line in Figure 4-4A shows the estimated travel times from the upstream detector. Using concurrent video to visually match every vehicle that stayed in the lane between the two stations, the points show the corresponding ground truth travel times. This process is repeated in Figure 4-4B at the downstream station. For the sake of comparison throughout this section, all plots of travel time are shown relative to vehicle arrival times at

downstream station. The performance of each detector station is summarized on the left-hand side of Table 4-1. Both estimates were, on average, within 10 percent of the true value while the corresponding naive link travel time estimates, presented in the center of the table, have an average error on the order of 25 percent.

Although the travel time estimation is not perfect, it is still quite good considering the fact that it is based on data from a single point in space. Looking closer at the data, Figure 4-5 shows a detail of the estimated trajectories implicit in the upstream travel time estimation. In this plot, the upstream detector is at zero feet and the downstream detector is at 1,800 feet. A total of 137 trajectories are shown, of which, 106 pass the downstream detector during the five minute period. The trajectories are not exact, e.g., no effort has been made to account for potential variance in u_C or the presence of lane change maneuvers, but the simple fact that they provide a good estimate of true travel time over an extended distance suggests that they are a good approximation. As further motivation, consider Figure 4-6. The methodology was used to estimate vehicle trajectories one half mile upstream and one half mile downstream of a detector station using data from the I-880 Field Experiment (Skabardonis et al., 1996), while the bold lines show actual probe vehicle trajectories over the same segment.

The trajectory approximations could be useful for planning applications or emissions modeling. For example, emissions are typically estimated using vehicle miles traveled, average velocity, average flow, or more recently, using point detectors capable of measuring instantaneous emissions from individual vehicles. But none of these methods are capable of capturing the effects of vehicle dynamics. As a result, significant factors contributing to vehicle emissions, such as acceleration, often go unmeasured (Holemen and Neimeier, 1998). On the other hand, a vehicle's dynamics are implicit in its trajectory and when used in conjunction with calibrated vehicle emissions (e.g., West et al., 1999), this work could allow for real time estimates of

emissions along an entire freeway. Future research will examine the accuracy of the trajectory estimates in terms of such applications.

4.2.2 Extending to Free Flow Conditions - a Long Example

During free flow traffic conditions, signals travel downstream with the vehicles and the transitions shown in Figure 4-2C should correspond to individual chords. Or, if we continue the assumption of constant signal velocities, they should now travel downstream at u_F. By erroneously assuming that free flow signals travel against the direction of travel with velocity u_C and treating the data the same way as congested periods, the travel time estimate will be based on the wrong set of vehicle observations. But, free flow traffic is characterized by approximately constant velocity over time and space. So the vehicles selected with u_C should have similar velocities to the correct set of vehicles and any resulting errors in the travel time estimate should be negligible.

Putting this hypothesis to the test, consider 24 hours of data between the same detector stations used in the previous example. This time, however, we arbitrarily present one of the lanes in the opposite direction. The two parts of Figure 4-7 show the estimated travel times from each detector station with a solid line. Manually generating ground truth matches for this long data set would be prohibitively time consuming. Instead, two vehicle reidentification algorithms are employed. For a given downstream measurement, each algorithm searches the upstream observations for the measurement that corresponds to the same vehicle (Coifman and Cassidy, 2001, Coifman, 2001). The resulting travel times for the matched vehicles are shown with points in each plot. As predicted, the estimation methodology performed quite well during free flow conditions, when the true travel time was on the order of 20 seconds.

Figure 4-8A shows a detail of the congested measurements. Again, the estimation method appears to follow the measured values while Figures 4-8B-C show the corresponding naive link travel time estimate using the local average velocity sampled every 30 seconds. As expected, the

fixed time samples do not provide a good estimator of link travel time, with some samples being over eight times too large.

4.2.3 Applying the methodology to conventional traffic data

The large errors from the naive estimate are due to the simple fact that a single 30 second sample at one point in space can not capture the travel time experienced by a vehicle traversing a link. Although the proposed methodology promises greater accuracy, most operating agencies would have to upgrade their hardware and/or software in the field to estimate travel time based on individual vehicle measurements. But the use of vehicle headways was chosen out of convenience. If a surveillance system only reports samples over fixed time periods and care is taken to measure space mean speed accurately, then the preceding theory is still valid and one can apply the estimation methodology to these data using a constant h, equal to the sampling period. In this scenario, the estimation methodology combines data from several fixed time samples rather than from individual vehicle measurements. The results for the short example using a 30 second sampling period are reported on the right hand side of Table 4-1. Note that the error is still less than half of that from the naive estimate.

4.2.4 Limitations

The estimation methodology assumes that *all* signals travel through the *entire* freeway link. This assumption fails when a queue partially covers a link. Unfortunately, the end of a queue can not be tracked using data from a single detector station.[3] Figure 4-9 shows two examples of this

[3] Daganzo (1997) presents a method to estimate the end of a queue between two detector stations using data from both stations. Used in conjunction with the present work, it could lead to better travel time and trajectory estimates; however, such work is beyond the scope of this paper, which focuses on extracting information from a single detector station.

failure. In each case, traffic over the downstream station is congested while vehicles at the upstream station are free flowing. Comparing the top and bottom halves of this figure, we see the upstream detector underestimates the travel time and the downstream overestimates it during these periods. Of course these errors would be reversed when the upstream end of the segment is queued while the downstream is free flowing. In any event, the periods where the method breaks down typically represent a small percentage of the day and as illustrated in this figure, they can be identified by differing estimates from either end of the link. Provided the estimates are transmitted to a central location, such as a Traffic Management Center, such comparisons would be easy to conduct.

Finally, one may have to assume a different flow-density relationship to apply this method at other locations. This modification could be as easy as calibrating the value of u_C, but if need be, one could extend the work to any flow density relationship in which flow is a strictly decreasing function of density in the congested regime.

4.3 Conclusions

Link travel time is considered to be more informative to users than flow, velocity, or occupancy measured at a point detector. This section has employed basic traffic flow theory to estimate link travel time using point detector data. Rather than simply measuring local velocity over fixed sample periods, the approach presented herein could be used to increase the "information" available from dual loop detectors and other vehicle detectors. The accuracy of the method lends further evidence that the linear approximation of flow density relationship is reasonable during congestion, supporting the work of Newell, Cassidy and others.

Since the method uses observations from a single point in space, changes in the traffic stream may be overrepresented or underrepresented, as illustrated in Figure 4-9. Because it is possible to estimate link travel time from either end of the link, the periods when the method breaks down can be identified easily. In contrast, vehicle reidentification techniques using data from more

than one detector station actually measure conditions over the link. Combining measured and estimated travel times, it should be possible to produce a robust incident detection system by looking for periods where the two approaches differ; perhaps even enabling incident detection during congested conditions. Naturally, such a system would have to account for recurring bottlenecks as well as normal queue growth and decay. To this end, future research will seek to extend the estimation methodology to inhomogeneous freeway links and improve performance during periods when a queue partially covers a link.

Although the estimation method is not perfect, it is surprisingly accurate for an approach that uses data from a single point in space. The estimated vehicle trajectories constructed en route, e.g., Figure 4-5, could be useful for applications such as quantifying vehicle emissions due to start/stop cycles on congested freeways.

Figure 4-1, Triangular flow density relationship showing the signal velocity during free flow, u_F, and congestion, u_C.

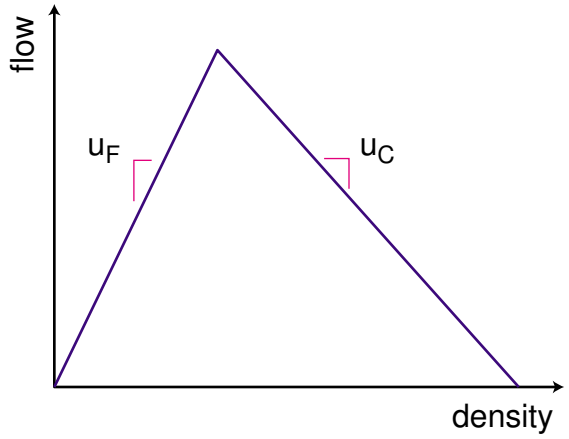

Figure 4-2, Time space diagram showing, (A) the chord for a vehicle passing the origin at 748 sec, (B) chords for subsequent vehicles, (C) truncated chords, (D) estimated trajectory and travel time for the vehicle in part A.

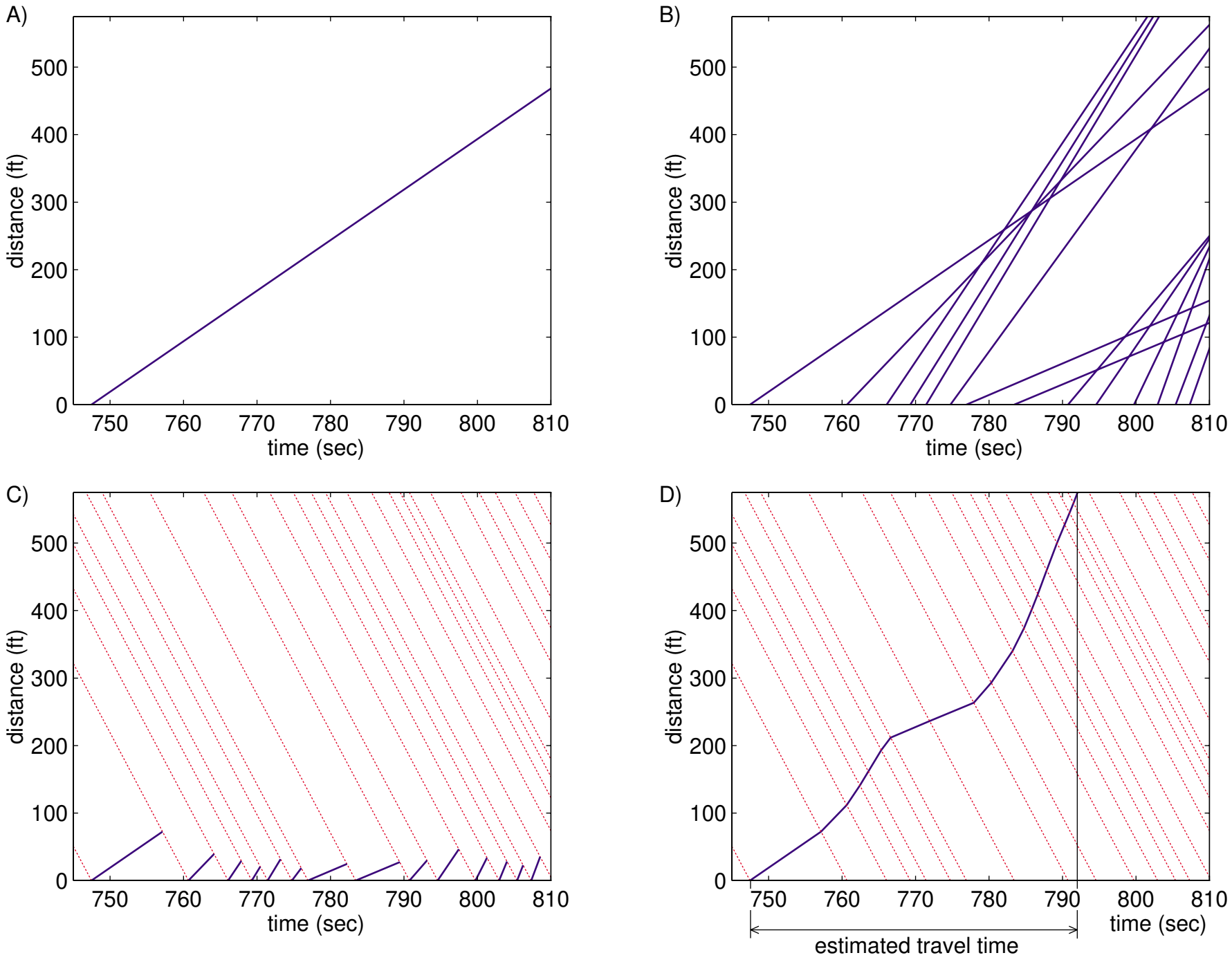

Figure 4-3, Schematic showing the relationships between signal velocity, u_C, vehicle velocity, v_j, headway, h_j, travel time, τ_j, and distance traveled, x_j, for a vehicle passing through band j.

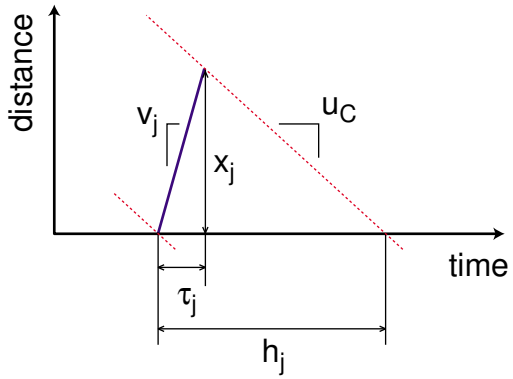

Figure 4-4, (A) Measured travel times (dots) and estimated from the upstream detector data (line), (B) repeated for the downstream detector data.

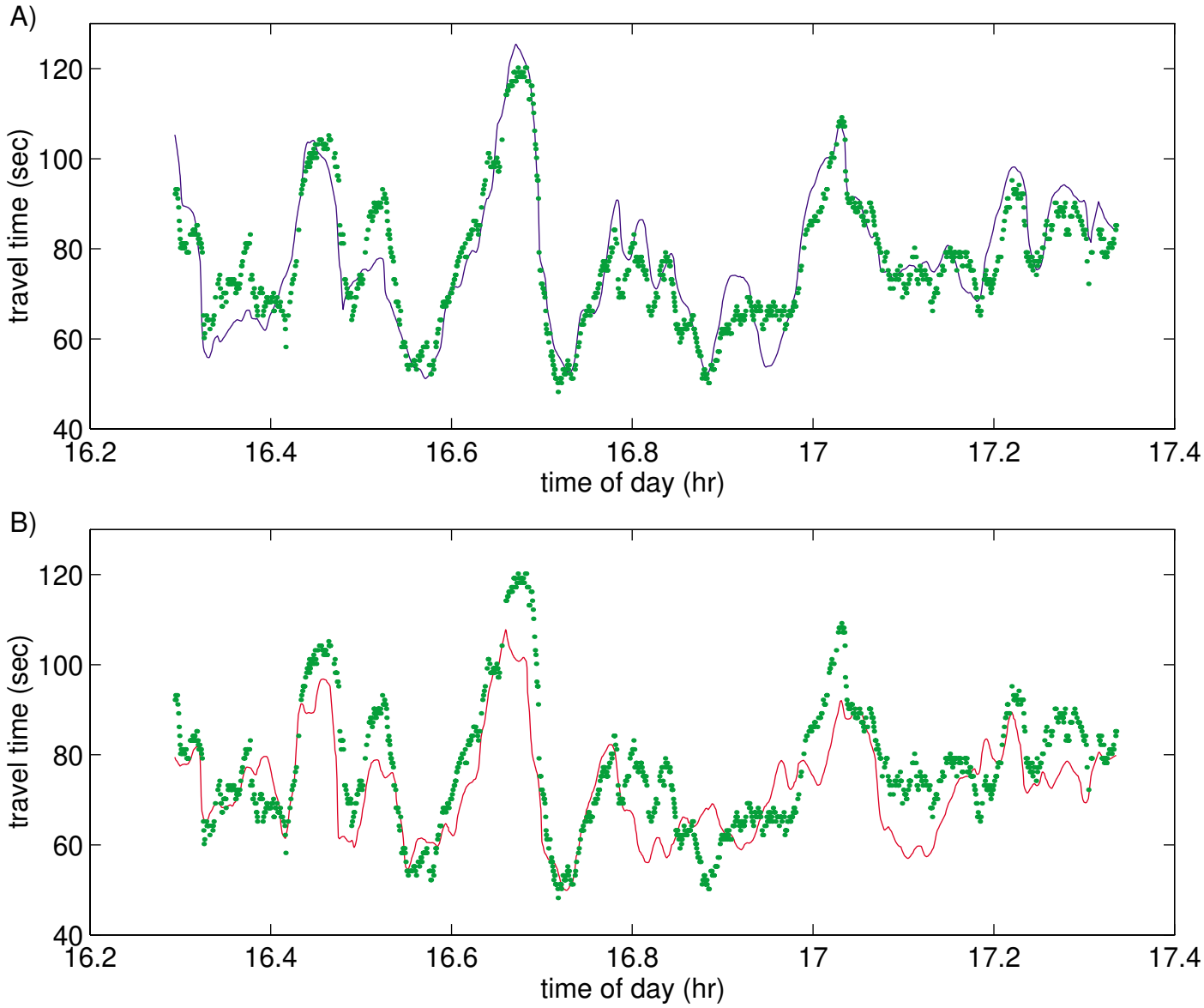

Figure 4-5, Detail from the estimated vehicle trajectories implicit in the travel time estimates of Figure 4A

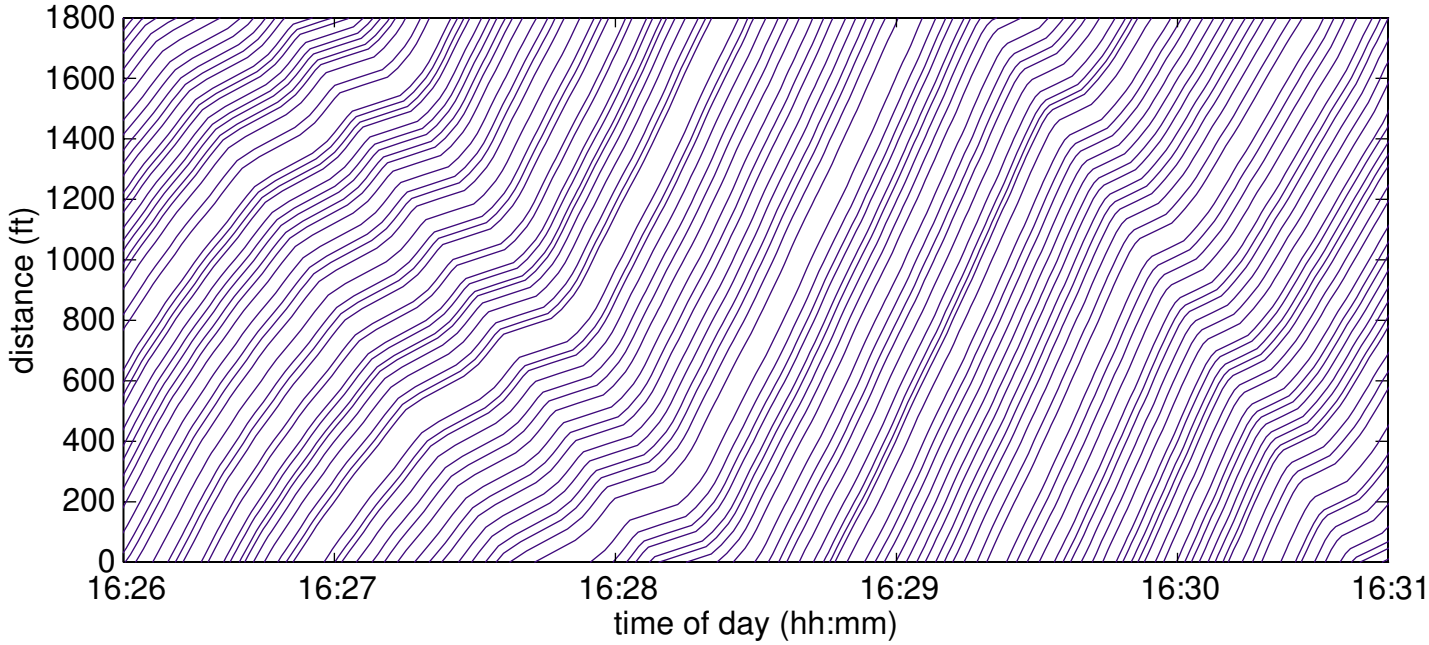

Figure 4-6, Estimated trajectories over one mile using data from a single detector station (at zero distance) and measured probe vehicle trajectories (shown with bold lines) for the same period.

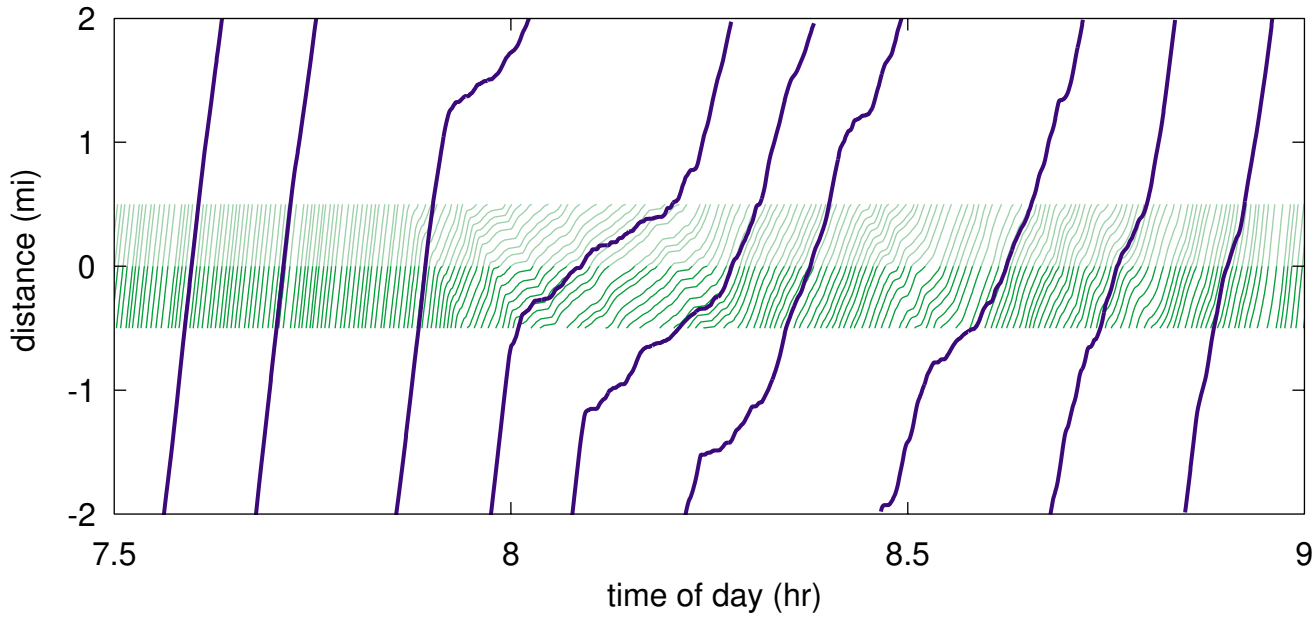

Figure 4-7, Measured travel times (dots) and estimated (line) from detector data over 24 hours, (A) upstream estimate (B) downstream estimate.

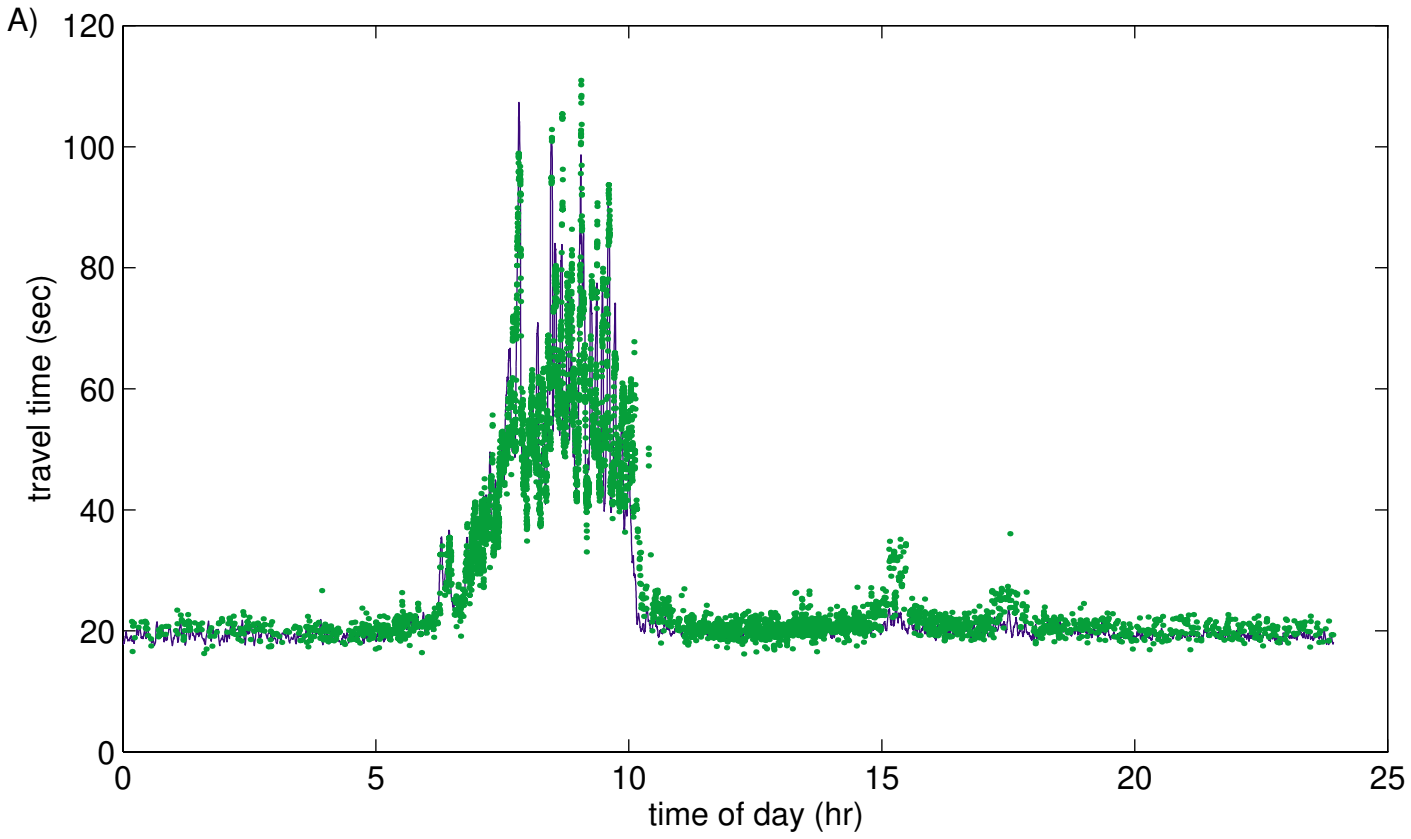

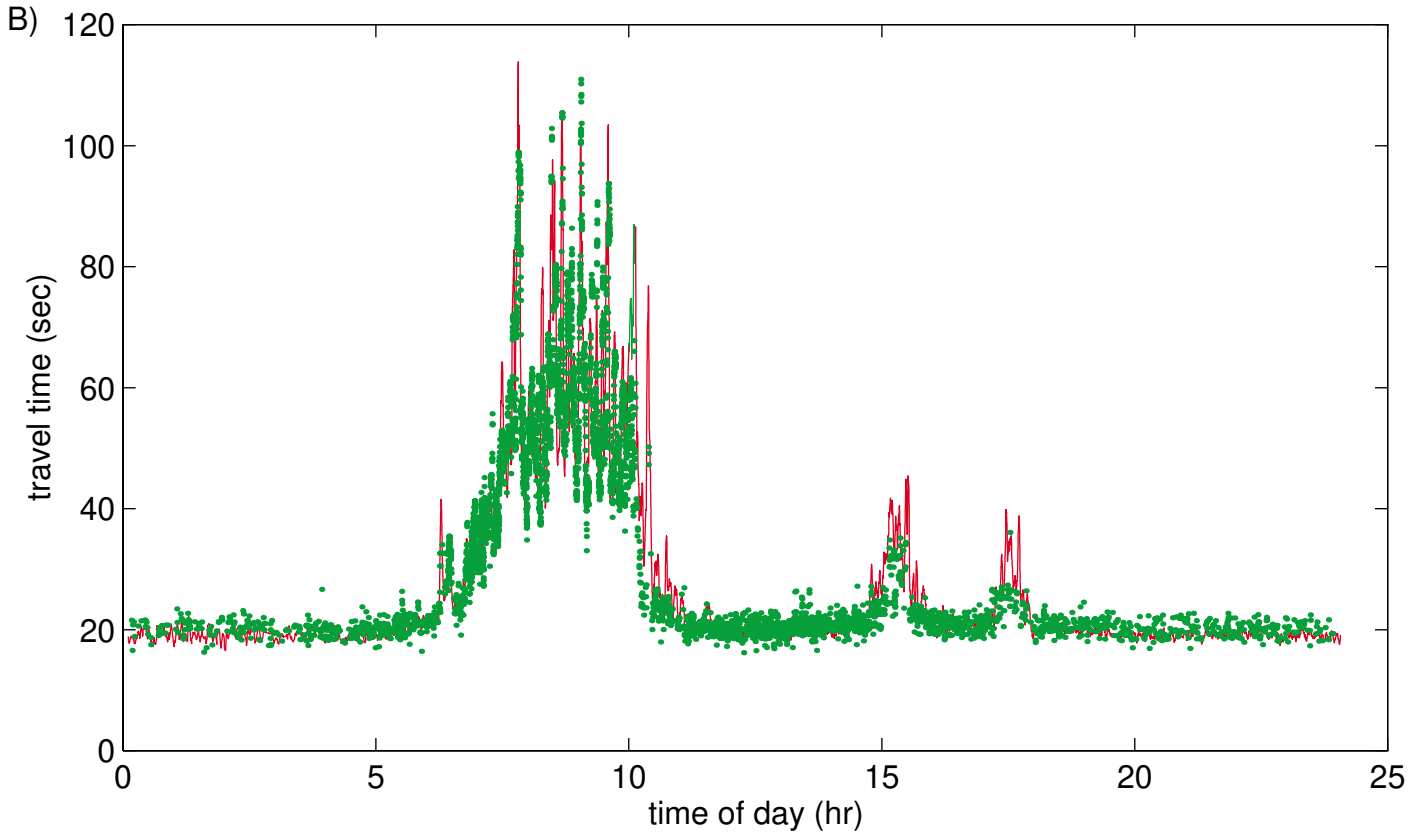

Figure 4-8, (A) Detail from Figure 7B, (B) the corresponding naive estimates taking the distance between detectors divided by 30 second average velocity downstream, (C) part B repeated with a larger vertical scale.

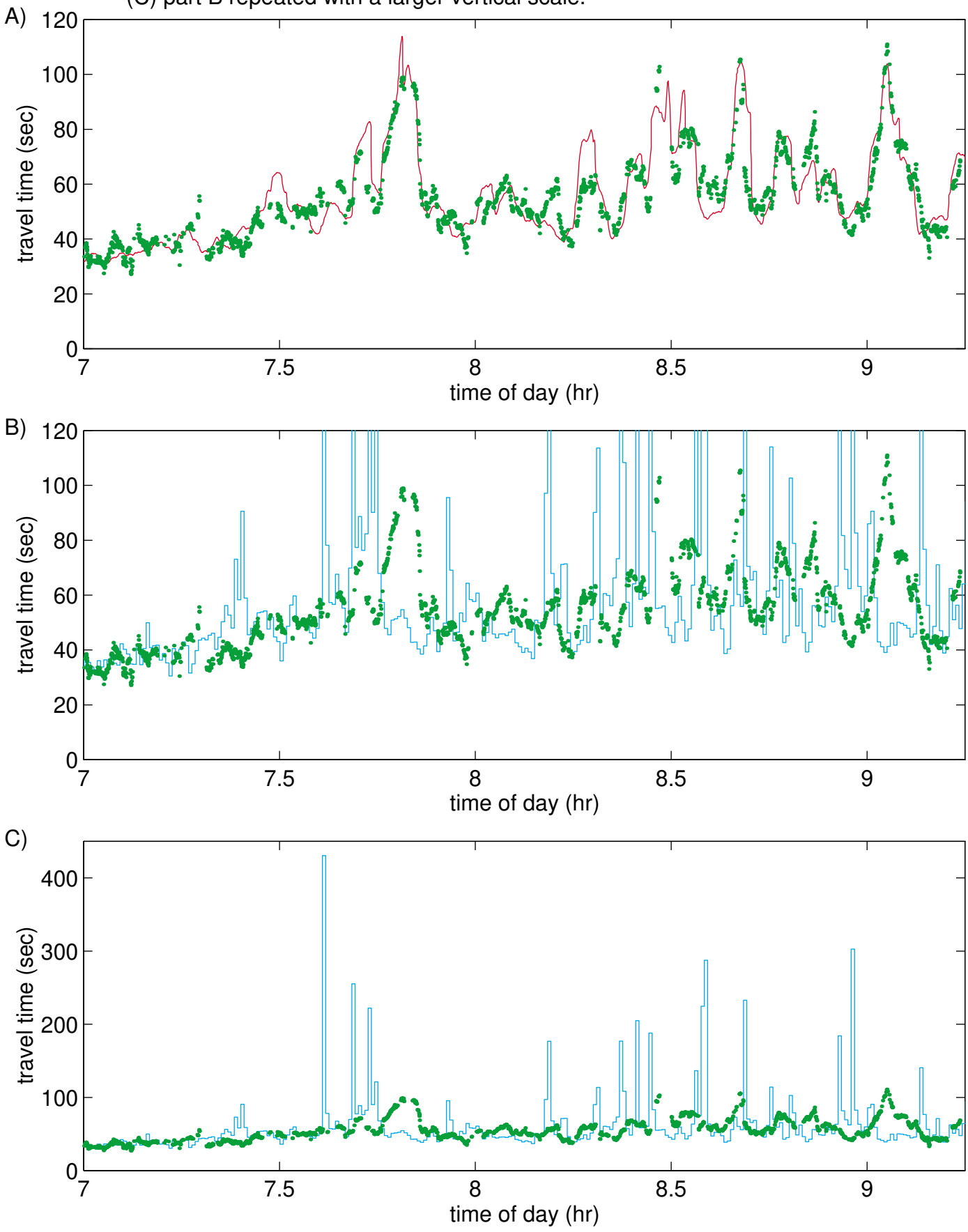

Figure 4-9, Examples where the estimation technique fails, (A)-(B) Details from Figure 7A and (C)-(D) corresponding details from Figure 7B.

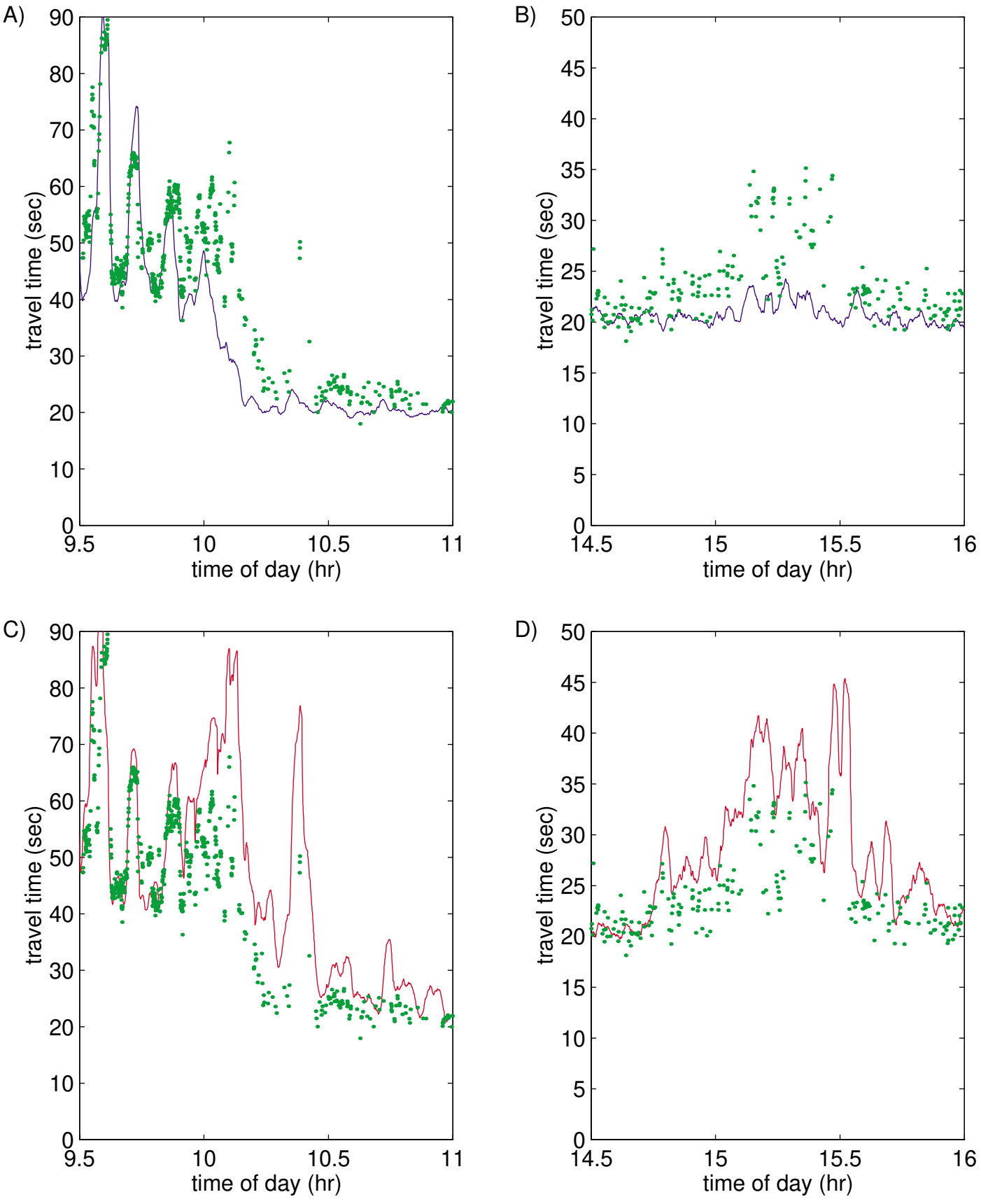

Table 4-1, Travel time estimation accuracy for the *short example*[a]

	Proposed estimate using measured headways		naive estimate		Proposed estimate using 30 second samples	
	upstream	downstream	upstream	downstream	upstream	downstream
average error (percent)	7	9.8	26.4	27.9	11.5	10.1
bias (sec)	0.6	-4.4	-0.2	-0.1	-2.8	-4.2

[a] Mean ground truth travel time is 77 seconds for this data set

5 EVENT-DATA BASED TRAFFIC DETECTOR VALIDATION TESTS

5.1 Introduction

Inductive loop detectors have been the preeminent vehicle detectors for the past several decades and most traffic surveillance applications depend on these detectors. Many operating agencies use specialized loop testers to assess the quality of the wiring (Kell et al., 1990, Ingram, 1976), but these tools bypass the controller and loop sensors; thus, they do not analyze the entire detector circuit, nor do they analyze the circuit in operation. To this end, most operating agencies employ simple heuristics such as, "Do the loop sensor indicator lights come on as a vehicle passes?" or simply, "Do the time series 30 second average flow and occupancy seem reasonable to the eye?" Such tests are typically employed when the loops are installed or when the quality of data coming from the detector station is questionable. These heuristics will catch severe errors and help diagnose them, but other problems can easily go unnoticed.

Many practitioners and some researchers (e.g., Jacobson et al., 1990, Cleghorn et al., 1991, Nihan, 1997), have worked to automate the latter heuristic by rephrasing the question, "Are the time series 30 second average flow and occupancy within statistical tolerance?" These systems often go undocumented in the literature because they are either designed in-house by an operating agency (see Chen and May, 1987 for examples) or were developed by a consulting firm using proprietary information. Because these automated systems only use aggregated data, they must accept a large sample variance and potentially miss problems altogether. For example, the systems have to tolerate a variable percentage of long vehicles in the sample population. As the percentage of long vehicles increases, the occupancy/flow ratio should increase simply because a long vehicle *occupies* the detector for more time compared to a shorter vehicle traveling at the same velocity (see section 2 for examples).

Chen and May (1987) developed a new approach for verifying detector data using event data, i.e., individual vehicle actuations. Their methodology examines the distribution of vehicles' *on-time*, i.e., the time the detector is occupied by a vehicle. Unlike conventional aggregate measures, their approach is sensitive to errors such as "pulse breakups", where a single vehicle registers multiple actuations because the sensor output flickers off and back on.

Coifman (1999) went a step further and compared the measured on-times from each loop in a dual loop detector on a vehicle by vehicle basis. At free flow velocities the on-times from the two loops should be virtually identical, even allowing for hard decelerations, regardless of vehicle length. Many hardware and software errors will cause the two on-times to differ. At lower velocities, vehicle acceleration can cause the two on-times to differ even though both loops are functioning properly and thus, congested periods were excluded from the analysis.

This section presents several new detector validation tests that employ event data to identify detector errors both at single loops and dual loop detectors. The tests are presented in terms of evaluating loop sensor units and detector validation, e.g., "if the data pass the test then the sensor can be trusted." The data are analyzed off-line, but the tests are simple enough that they could be implemented in real-time to identify detector errors in real time and most of them could be used to actively *clean* incoming data from a traffic surveillance system.

After presenting the basic data collection and measurement, this section presents eight different detector validation tests. Five of these tests can be applied to single loop detectors or non-invasive sensors that aggregate data using similar techniques, while all of the tests can be applied to dual loop detectors.

5.2 The data

The work uses event data collected from dual loop detector stations in the Berkeley Highway Laboratory along Interstate-80, north of Oakland, CA to demonstrate the tests (Coifman et al., 2000). The following five sensor units are evaluated in this study,

Peek GP5 revision E (GP5-E),

Peek GP5 revision G (GP5-G),

Peek GP6 revision C (GP6),

Eberle Design Inc. LM222 (EDI),

Intersection Development Corporation Model 222 (IDC).

Except where noted, the study uses 24 hours of data from one dual loop detector for each sensor unit. The date and detector were chosen at random, but all of the loop detector stations were evaluated thoroughly to identify and exclude any hardware problems. Table 5-1 summarizes the number of vehicles observed in each of these data sets, aggregated into three velocity ranges. To correct for any measurement errors, the exact criteria used to determine which velocity range a vehicle falls in is described in subsection 5.3.1.

Table 5-1 Number of vehicles in each sample

Data file	# veh > 45mph	# veh 20-45 mph	# veh < 20mph	Total # veh
EDI	20251	4697	2309	27257
GP6	20362	1320	2636	24318
GP5-G	19802	2254	292	22348
IDC	20711	3096	2155	25962
GP5-E	18825	5083	2147	26055

5.2.1 Vehicle measurements

This research used conventional model 170 controllers to collect the event data at 60 Hz. The process is illustrated in Figure 5-1A, a time-space diagram depicting a vehicle passing over a dual loop detector. The controller normally records four transitions, i.e., the turn-on and turn-off

times at each of the loops, as shown in Figure 5-1B. Integral to these measurements is the process of matching pulses between the paired loops. For this study, each pulse at the second loop is matched to the most recent pulse at the first loop that preceded it. When the dual loop detector is operating properly, two successive pulses rarely come from one loop without an intervening pulse on the other loop (the loops are typically spaced close enough to ensure that one vehicle will actuate both loops before the next vehicle actuates the upstream loop). The error detection strategy is sensitive to unmatched pulses and it will detect when this assumption breaks down.

After matching pulses between loops, the following parameters are calculated for each vehicle: dual loop traversal time via the rising edges, TT_r, dual loop traversal time via the falling edges, TT_f, total on-time at the first loop, OT_1, and total on-time at the second loop, OT_2, as indicated in Figure 5-1. These data yield two measured of individual vehicle velocity:

$$V_r = (\text{loop separation}) / TT_r \tag{5-1}$$

$$V_f = (\text{loop separation}) / TT_f \tag{5-2}$$

and these measurements are used calculate two measurements of effective vehicle length,

$$L_1 = OT_1 * V_r \tag{5-3}$$

$$L_2 = OT_2 * V_f \tag{5-4}$$

In the case of single loop detector tests, the work uses the second loop in the dual loop detector and estimates velocity using the median of 11 OT_2 measurements centered on the given vehicle (see section 3),

$$V_{est} = 20 \text{ feet} / \text{median}(OT_2) \tag{5-5}$$

and then, these estimated velocities can be used to estimate effective vehicle length,

$$L_{est} = OT_2 * V_{est} \tag{5-6}$$

Finally, whether using both loops or a single loop, the vehicle headway, H, is measured from the difference between on_2 from two consecutive vehicles.

5.3 Traffic Detector Validation tests

5.3.1 Individual vehicle velocity versus moving median velocity test

As the title suggests, this test compares individual vehicle velocity against the median of 11 velocity measurements centered on the given vehicle. If the velocity of the vehicle deviates from the median by more than a preset threshold, (set to 20 mph in this analysis), the individual velocity measurement is considered erroneous.

When these errors are encountered, it could result in the vehicle being classified in an incorrect velocity range. So the moving median of V_r is used to select the velocity range in all of the tables. To illustrate the power of this filter, Figure 5-2 compares the measured velocities and the moving median velocities from the GP5-G sensor, the worst case observed in our data sets. As can be seen from the figure, the median velocities filter out much of the noise from the raw data. In real-time analysis, one may not be able to afford the lag time necessary to observe all of the following vehicles, so the research also considered a moving restricted to observations that preceded the current vehicle. As expected, performance was not as good as the results presented here, but it still proved beneficial.

Tables 5-2A and 5-2B present the statistics after applying this test to each day of data from the different sensor units using velocity from the rising and falling edge, respectively. For reference, the results are ranked from 1 (best) to 5 (worst) in each table. The falling edge from the GP5-G sensor unit stands out as clearly being poorer than the other sensors. As noted in section 3, Equation 5-5 is an estimate of median velocity, so the comparison can be repeated using the measured velocity across loops and the estimated velocity from a single loop, i.e., the test checks whether the on-times are consistent with the measured velocities. These results are presented in

Tables 5-2C and 5-2D, for the subject data sets and they are similar to Tables 5-2A and 5-2B. One notable difference is that the EDI sensor shows slightly diminished performance when using the estimates and this result is consistent with the outcome of later tests that will be presented. Finally, although not shown here, the test can be repeated using estimated data from the other detector.

Table 5-2A Percentage of vehicles passing the median velocity test using V_r versus moving_median(V_r)

Data File	% acceptable (> 45 mph)	% acceptable (20-45 mph)	% acceptable (< 20 mph)	% acceptable all vehs.	Rank
EDI	99.8%	100.0%	99.9%	99.8%	2
GP6	99.9%	100.0%	100.0%	99.9%	1
GP5-G	99.8%	99.8%	100.0%	99.8%	2
IDC	99.9%	100.0%	100.0%	99.9%	1
GP5-E	99.9%	100.0%	100.0%	99.9%	1

Table 5-2B Percentage of vehicles passing the median velocity test using V_f versus moving_median(V_f)

Data File	% acceptable (> 45 mph)	% acceptable (20-45 mph)	% acceptable (< 20 mph)	% acceptable all vehs.	Rank
EDI	98.7%	99.7%	99.8%	99.0%	4
GP6	99.9%	100.0%	100.0%	99.9%	1
GP5-G	78.7%	95.1%	100.0%	80.9%	5
IDC	99.7%	100.0%	100.0%	99.8%	2
GP5-E	99.2%	99.9%	100.0%	99.4%	3

Table 5-2C Percentage of vehicles passing the median velocity test using V_r versus V_{est}

Data File	% acceptable (> 45 mph)	% acceptable (20-45 mph)	% acceptable (< 20 mph)	% acceptable all vehs.	Rank
EDI	92.7%	100.0%	99.8%	94.4%	5
GP6	99.6%	94.6%	100.0%	99.3%	3
GP5-G	99.0%	98.2%	99.7%	98.9%	4
IDC	99.7%	98.3%	99.8%	99.4%	1
GP5-E	99.6%	96.8%	99.7%	99.3%	2

Table 5-2D Percentage of vehicles passing the median velocity test using V_f versus V_{est}

Data File	% acceptable (> 45 mph)	% acceptable (20-45 mph)	% acceptable (< 20 mph)	% acceptable all vehs.	Rank
EDI	95.1%	99.7%	99.7%	96.1%	4
GP6	99.6%	94.9%	100.0%	99.2%	2
GP5-G	78.2%	90.4%	99.7%	80.2%	5
IDC	99.1%	98.5%	99.8%	99.0%	3
GP5-E	99.4%	97.0%	99.7%	99.2%	1

5.3.2 Headway versus on-time test

Figure 5-3A shows the measured H versus OT_2 from the GP6 data. These data were grouped into free flow and congested groups based on V_r > 45 mph. Relatively short on-times and occasional long headways characterize the free flow data, while occasional long on-times characterize the congested data. After reviewing many such plots, we defined two regions of the headway on-time plane that should contain all free flow observations or all congested observations, as shown in Figure 5-3B. The free flow region is bounded by OT_2 < 0.3 sec and H > 8 sec, while the congested region is bounded by OT_2 > 1.3 sec. Of course most observations under either condition will fall somewhere between these two regions.

This traffic flow characterization can be utilized in detecting certain errors at single loop detectors, e.g., if a measurement falls in the free flow region but V_{est} < 45 mph or conversely if a measurement falls in the congested region but V_{est} > 45 mph. Table 5-3 summarizes the results of this test applied to each of the data sets. Very few errors were found for these sets, but as noted previously, the detector hardware was verified to be in full functioning order before the tests were applied. Finally, one could modify this test to use measured velocity at dual loop detectors.

Table 5-3 Percentage of vehicles passing the headway on-time test

Data File	% FF median_vel & FF region in h-o plane	% FF median_vel & Cong. Region in h-o plane	% Cong. Median_vel & FF region in h-o plane	% Cong. Median_vel & Cong region in h-o plane	Rank
EDI	5.1%	0.0%	0.0%	0.9%	5
GP6	5.4%	0.0%	0.0%	2.2%	1
GP5-G	6.9%	0.0%	0.0%	0.5%	2
IDC	5.4%	0.0%	0.0%	1.6%	4
GP5-E	5.1%	0.0%	0.0%	2.1%	3

5.3.3 Feasible range of vehicle lengths test

There exists some finite range of feasible vehicle lengths and this research assumes feasible effective vehicle lengths to range between 10 ft and 90 ft. If a measured vehicle length falls outside of this range, it would indicate a detector error. The test can be applied to estimated or measured lengths, thereby providing a test for both single and dual loop detectors. If the individual length is too short, it may be indicative of pulse break-ups, a sensor set to pulse mode rather than presence mode, or similar errors. On the other hand, if the individual length is too long, it may be due to the detector sticking on after the passing of the vehicle.

Tables 5-4A through 5-4C present the statistics after applying this test to each data set using L_1, L_2, and L_{est}, respectively. As with the previous test, very few errors were found in these sets, but they should be able to identify chronic errors. As with Tables 5-2C and 5-2D, the EDI does demonstrate slightly worse performance than the other sensors.

Table 5-4A Percentage of vehicles passing the feasible length test using L_1

Data File	% acceptable (> 45 mph)	% acceptable (20-45 mph)	% acceptable (< 20 mph)	% acceptable all vehs.	Rank
EDI	98.1%	98.7%	98.1%	98.2%	5
GP6	99.7%	99.7%	100.0%	99.8%	2
GP5-G	99.9%	99.9%	99.3%	99.9%	1
IDC	99.8%	99.7%	99.9%	99.8%	3
GP5-E	99.7%	99.7%	99.8%	99.7%	4

Table 5-4B Percentage of vehicles passing the feasible length test using L_2

Data File	% acceptable (> 45 mph)	% acceptable (20-45 mph)	% acceptable (< 20 mph)	% acceptable all vehs.	Rank
EDI	97.4%	98.2%	98.0%	97.5%	5
GP6	99.7%	99.7%	100.0%	99.7%	2
GP5-G	98.8%	99.2%	99.7%	98.9%	4
IDC	99.8%	99.8%	99.9%	99.8%	1
GP5-E	99.6%	99.8%	99.9%	99.6%	3

Table 5-4C Percentage of vehicles passing the feasible length test using L_{est}

Data File	% acceptable (> 45 mph)	% acceptable (20-45 mph)	% acceptable (< 20 mph)	% acceptable all vehs.	Rank
EDI	99.1%	99.3%	98.0%	99.1%	5
GP6	99.6%	99.6%	99.5%	99.6%	1
GP5-G	99.6%	99.6%	99.0%	99.6%	2
IDC	99.5%	99.7%	98.6%	99.4%	4
GP5-E	99.5%	99.5%	99.3%	99.5%	3

5.3.4 Feasible range of headway and on-time tests

As with vehicle length, there are physical limits on feasible headways and on-times. These parameters can be used to detect chronic errors at single and dual loop detectors. This research assumes a minimum feasible headway of 0.75 sec and minimum on-time of 0.16 sec. During free flow conditions, one can also apply a maximum feasible on-time. An 80 ft vehicle traveling at 45 mph should have an on-time of approximately 1.2 sec. Adding an error margin of 0.1 sec, a detector observing many free flow vehicles with on-times greater than 1.3 sec would be suspect.

Tables 5-5A through 5-5D present the statistics after applying these tests to each data set. The EDI has more short headways and on-times than the other sensors. Coifman (1999) has already found that these sensor units are prone to flicker.

Table 5-5A Percentage of vehicles with $H > 0.75$ sec.

Data File	% acceptable (> 45 mph)	% acceptable (20-45 mph)	% acceptable (< 20 mph)	% acceptable all vehs.	Rank
EDI	92.1%	99.2%	100.0%	94.0%	5
GP6	96.6%	98.6%	100.0%	97.1%	2
GP5-G	96.3%	99.0%	100.0%	96.6%	3
IDC	94.9%	99.6%	100.0%	95.9%	4
GP5-E	96.2%	99.5%	100.0%	97.2%	1

Table 5-5B Percentage of vehicles with $OT_2 > 0.16$ sec.

Data File	% acceptable (> 45 mph)	% acceptable (20-45 mph)	% acceptable (< 20 mph)	% acceptable all vehs.	Rank
EDI	74.8%	99.5%	99.7%	81.2%	5
GP6	97.6%	99.7%	100.0%	97.9%	1
GP5-G	95.4%	99.9%	100.0%	95.9%	3
IDC	96.8%	99.9%	100.0%	97.4%	2
GP5-E	93.6%	99.7%	100.0%	95.3%	4

Table 5-5C Percentage of vehicles with $H > 0.75$ sec and $OT_2 > 0.16$ sec.

Data File	% acceptable (> 45 mph)	% acceptable (20-45 mph)	% acceptable (< 20 mph)	% acceptable all vehs.	Rank
EDI	68.0%	98.7%	99.7%	76.0%	4
GP6	94.3%	98.4%	100.0%	95.2%	1
GP5-G	91.9%	98.9%	100.0%	92.7%	3
IDC	91.9%	99.5%	100.0%	93.4%	2
GP5-E	90.2%	99.3%	100.0%	92.7%	3

Table 5-5D Percentage of free flow vehicles with $OT_2 < 1.3$ sec.

Data File	% acceptable (> 45 mph)	Rank
EDI	100.0%	1
GP6	100.0%	1
GP5-G	99.9%	2
IDC	100.0%	1
GP5-E	100.0%	1

5.3.5 Length differences and ratios at dual loop detectors

Coifman (1999) used the difference between OT_1 and OT_2 to assess the performance of a dual loop detector during free flow condition. These tests were constrained by the fact that at lower velocities, acceleration can cause an on-time difference even though the loop detectors are

functioning properly. Unfortunately, this constraint precludes the earlier test from identifying errors that only occur during congested conditions. In response to this limitation, this new test uses the difference between L_1 and L_2 to control for velocity and extend the test into congested conditions. Of course some errors may be correlated to vehicle length as well, so a second version of the test is used to normalize for length, i.e., $(L_1 - L_2) / (L_1 + L_2)$. If the sensors are functioning properly, these differences should be close to zero.

Table 5-6A summarizes the results for $L_1 - L_2$. To facilitate collection and analysis, the data were aggregated into bins by 0.5 ft, so the central bin represents a range of +/- 3 in, and the central three bins span +/- 9 in. Similarly, Table 5-6B summarizes the results for $(L_1 - L_2) / (L_1 + L_2)$ aggregated into bins of size 0.003. Thus, the central bin represents a range of +/- 0.0015 and the central three bins span +/- 0.0045. In both tables and all velocity ranges, the GP5-G performs the worst out of all of the sensors. These results are consistent with the results during free flow found in Coifman (1999). Also note that the EDI sensor performs almost as bad as the GP5-G in the second test but not the first, indicating a vehicle length bias in the EDI's errors.

Table 5-6A Percentage of vehicles passing the L_1-L_2 test.

Data File	% central bin			% central 3 bins			% central bin all vehs	% central 3 bins all vehs	Rank
	> 45mph	20-45mph	< 20mph	> 45mph	20-45mph	< 20mph			
EDI	70.7%	84.5%	66.9%	92.7%	95.8%	88.4%	72.8%	92.9%	4
GP6	89.9%	93.1%	87.8%	94.4%	95.5%	93.2%	89.9%	94.3%	1
GP5-G	62.1%	50.7%	63.5%	72.5%	69.2%	87.2%	60.8%	72.2%	5
IDC	88.6%	92.6%	85.4%	94.0%	95.5%	93.1%	88.8%	94.1%	2
GP5-E	85.4%	90.2%	83.9%	92.1%	94.2%	92.9%	86.2%	92.5%	3

Table 5-6B Percentage of vehicles passing the $(L_1$-$L_2)/(L_1+L_2)$ test.

Data File	% central bin			% central 3 bins			% central bin all vehs	% central 3 bins all vehs	Rank
	> 45mph	20-45mph	< 20mph	> 45mph	20-45mph	< 20mph			
EDI	51.9%	36.4%	22.1%	60.2%	67.6%	51.8%	46.8%	60.8%	4
GP6	72.7%	77.8%	67.7%	87.9%	92.0%	85.4%	72.5%	87.8%	1
GP5-G	40.3%	27.8%	28.8%	56.1%	45.0%	56.9%	38.7%	54.8%	5
IDC	71.1%	75.4%	63.2%	86.2%	91.3%	83.2%	70.9%	86.6%	2
GP5-E	58.4%	62.5%	51.2%	78.6%	86.6%	78.2%	58.6%	80.1%	3

5.3.6 Cumulative distribution of vehicle lengths

It may not be feasible to calculate the vehicle length differences in Tables 5-6A and 5-6B, either due to limited processing power in the controller or when working with single loop detectors. In these cases, it is possible to calculate the cumulative distribution function (CDF) of the measured or estimated lengths, and summarized by the deciles of the distribution. Of course the CDF will capture site specific phenomena, such as the percentage of large trucks, so it is not feasible to specify a universally "good" range for this distribution. But it is possible to compare the CDF measured one day with that measured during the same time period on the next day. Thereby allowing an agency to detect sudden changes in detector performance. It is also possible to compare the CDF from one detector station to that at the next detector station on the roadway to control for day to day variance. Figure 5-4A illustrates such a comparison using L_1. This plot shows the daily CDF of L_1 in a single lane, over five days at one detector station and seven days in the same lane at a second detector station, 1/3 mi away. All of these data were recorded with a GP5-E sensor unit except for one of the days at the second station, which were recorded using an EDI sensor unit. Aside from some variability in the percentage of long vehicles, all of the curves from the GP5-E sensors fall on top of each other. The curve from the EDI sensor is distinct from the other curves and indicates that the sensor is recording many more "short vehicles". As mentioned previously, these sensors tend to flicker and the short length measurements are simply due to detector errors. This plot shows that one can compare across days and nearby locations reliably. The process is repeated using the corresponding estimated lengths in Figure 5-4B. This time, however, the curves only show the deciles. Unfortunately, the problem with the EDI cards impact both the on-time and the median on-time. Since the estimate is proportional to the former and inversely proportional to the latter, the problem is less pronounced in this plot, but it is still evident.

5.3.7 Loss of a loop in a dual loop detector

One loop in a dual loop detector may stick on or stick off while the other loop continues working. It is a simple test to count the number of pulses at one loop since the last pulse at the other loop and quickly identify when these errors occur. For example, if the controller sees five pulses at the second loop since the last pulse at the first loop, it could respond by resetting the sensor card, sending an alarm, and/or treating the remaining loop in the dual loop as a single loop detector.

5.3.8 Counting the number of consecutive congested samples

This test is intended for single and dual loop detectors. It takes samples of 10 consecutive vehicles and applies Equation 5-5 to estimate the velocity. The test assumes that traffic becomes congested whenever this estimate drops below 40 mph for four consecutive samples, the last of which is explicitly marked as being congested. The four samples are used to eliminate transient errors due to an unusually large number of long vehicles during free flow conditions. The test then assumes that traffic remains congested until it sees a single sample of 50 mph. The higher threshold is used to prevent frequent transitions when the true velocity is near the threshold velocity. The test keeps track of how many congested samples precede each free flow sample. Based on the criteria, one would expect that most free flow samples would be preceded by another free flow sample, i.e., zero congested samples, but some will be preceded by many congested samples. To quantify this test, the distribution is calculated, e.g., Figure 5-5. There should be few free flow samples that are preceded by few congested samples, if this is not usually the case, then it would be indicative of a detector error.

5.4 Conclusions

This section has presented eight detector validation tests using event data. Five of these tests can be applied to single loop detectors. Some of the tests are quite simple, such as the loss of a loop

in a dual loop detector, while other tests are more involved, such as the length differences at dual loops, which extends our earlier work with dual loop detectors to non-free flow conditions.

In most cases, the tests were presented without explicit criteria to distinguish between good and bad sensors. This deliberate omission is due both to the fact that such parameters depend on the required accuracy from the loop detectors, and because the event data used in this study are uncommon. The authors know of only a few locations where such data have been collected, making it difficult to provide universal guidelines for deploying such tests. The section provides enough guidance to assist a practitioner in assessing the usefulness of a given test and the first steps toward implementing it if it appears promising. As such, additional calibration may be necessary, but it should not be difficult to conduct.

The tests were used to contrast the performance of different sensor models and most of the tests have been presented using 24 hr blocks of data. In practice, they can also be used to identify permanent and transient hardware problems in other components of the detection system, e.g., cross talk between loops or a short in the lead wires that only materializes in the rain. For operational implementation, the tests could be applied hourly or after a fixed number of vehicles pass. Some of the tests can even be used to clean up erroneous measurements, such as the individual vehicle velocity versus moving median test, which was used to replace transient errors with median values from adjacent measurements. Other tests, such as the feasible length test, could be used to exclude individual vehicle measurement errors from aggregate parameter calculations such as flow and occupancy.

Figure 5-1 One vehicle passing over a dual loop detector, (A) the two detection zones and the vehicle trajectory as shown in the time space plane. The height of the vehicle's trajectory reflects the non-zero vehicle length. (B) The associated turn-on and turn-off transitions at each detector.

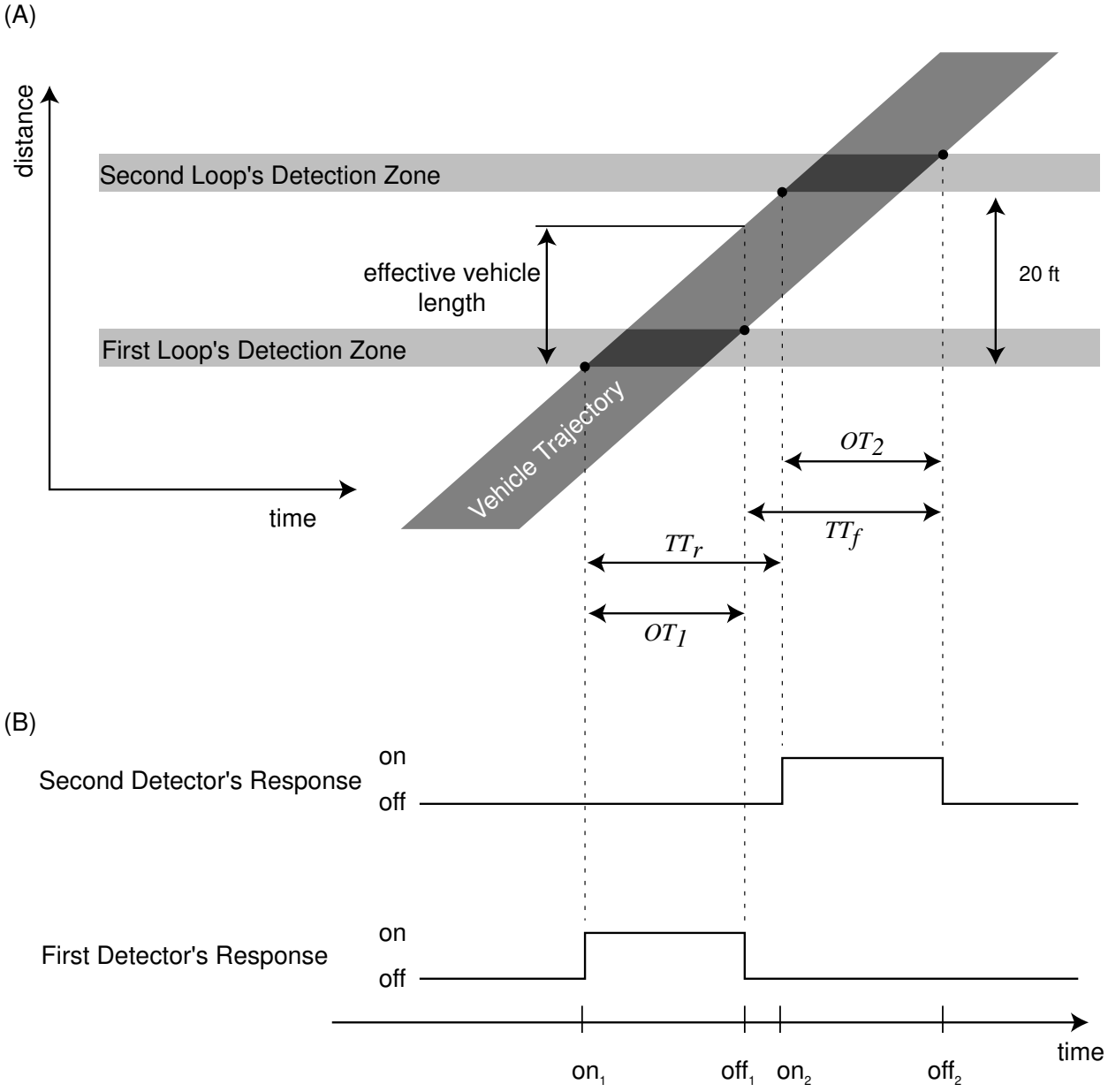

Figure 5-2 (A) Individual V_f from the GP5-G, (B) moving median of the data from part A.

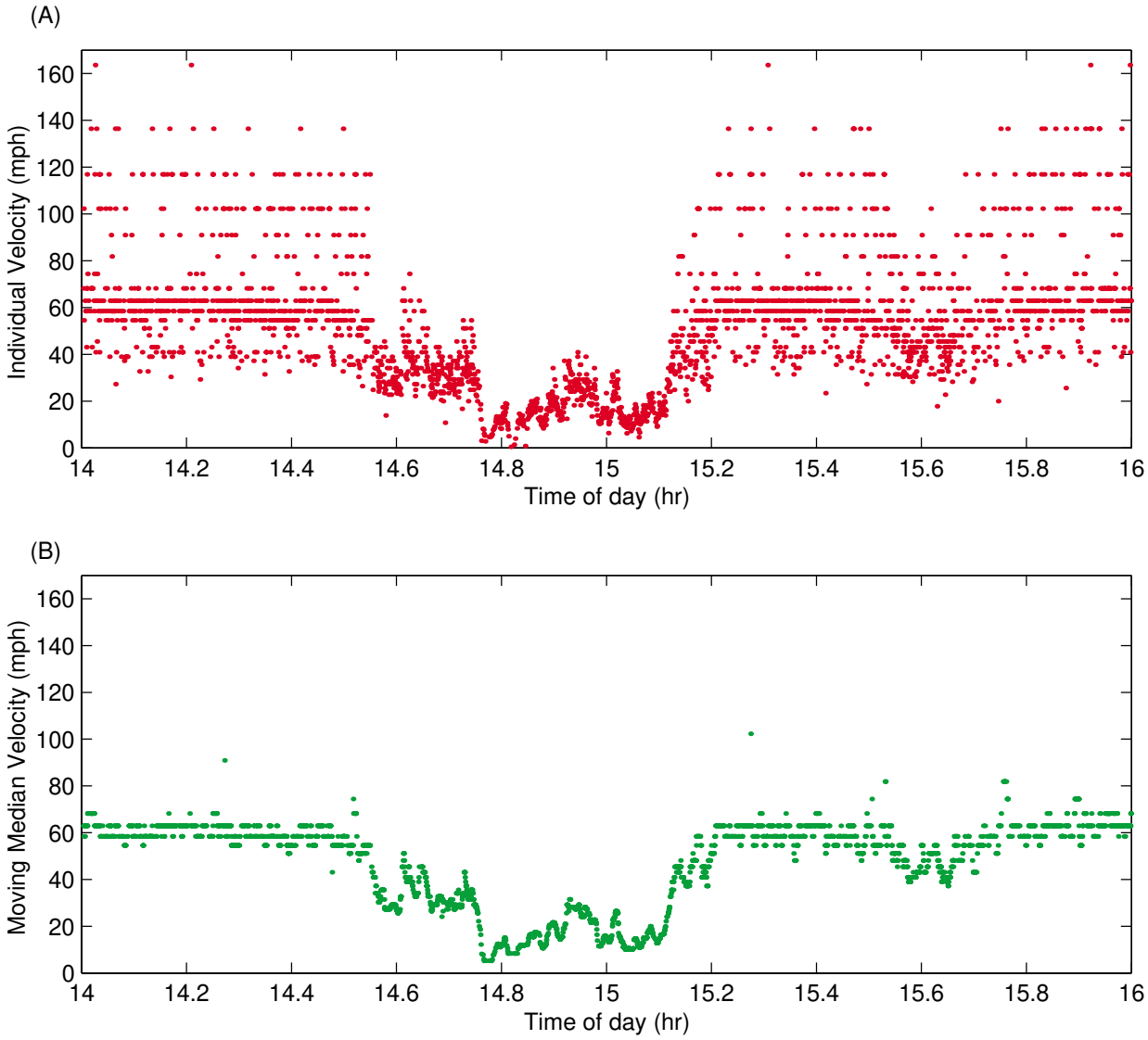

Figure 5-3 (A) Measured H versus OT_2 from the GP6 data using $V_r > 45$ mph to identify the free flow data, (B) regions of the headway on-time in which measurements should all be free flow or all non-free flow, i.e., congested.

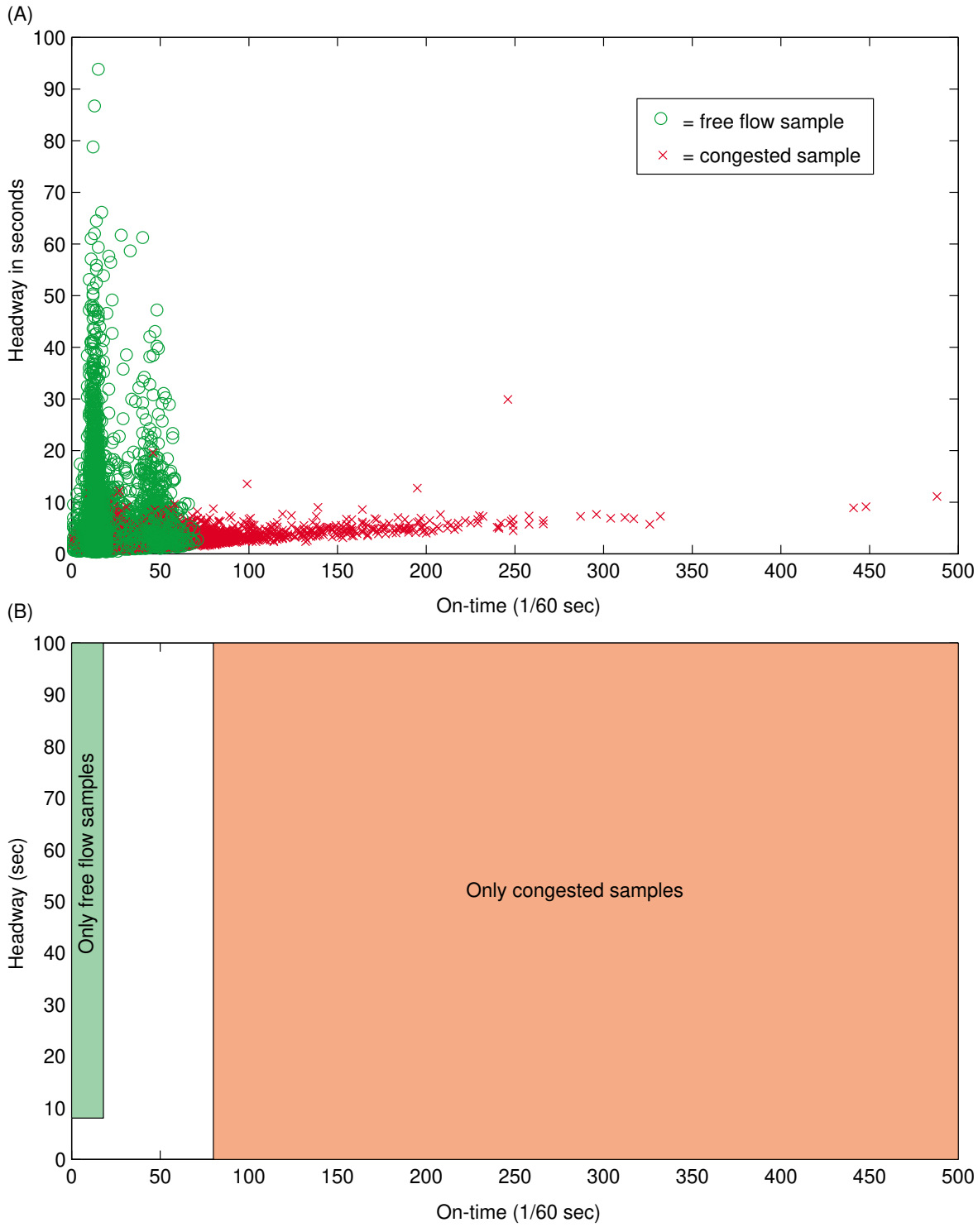

Figure 5-4 Five days of data from one detector station and six days of data from another station 1/3 mile away, both using GP5-E sensor units. Also one day from the second station an EDI sensor unit, (A) Cumulative Distribution of L_1, (B) deciles of L_{est}

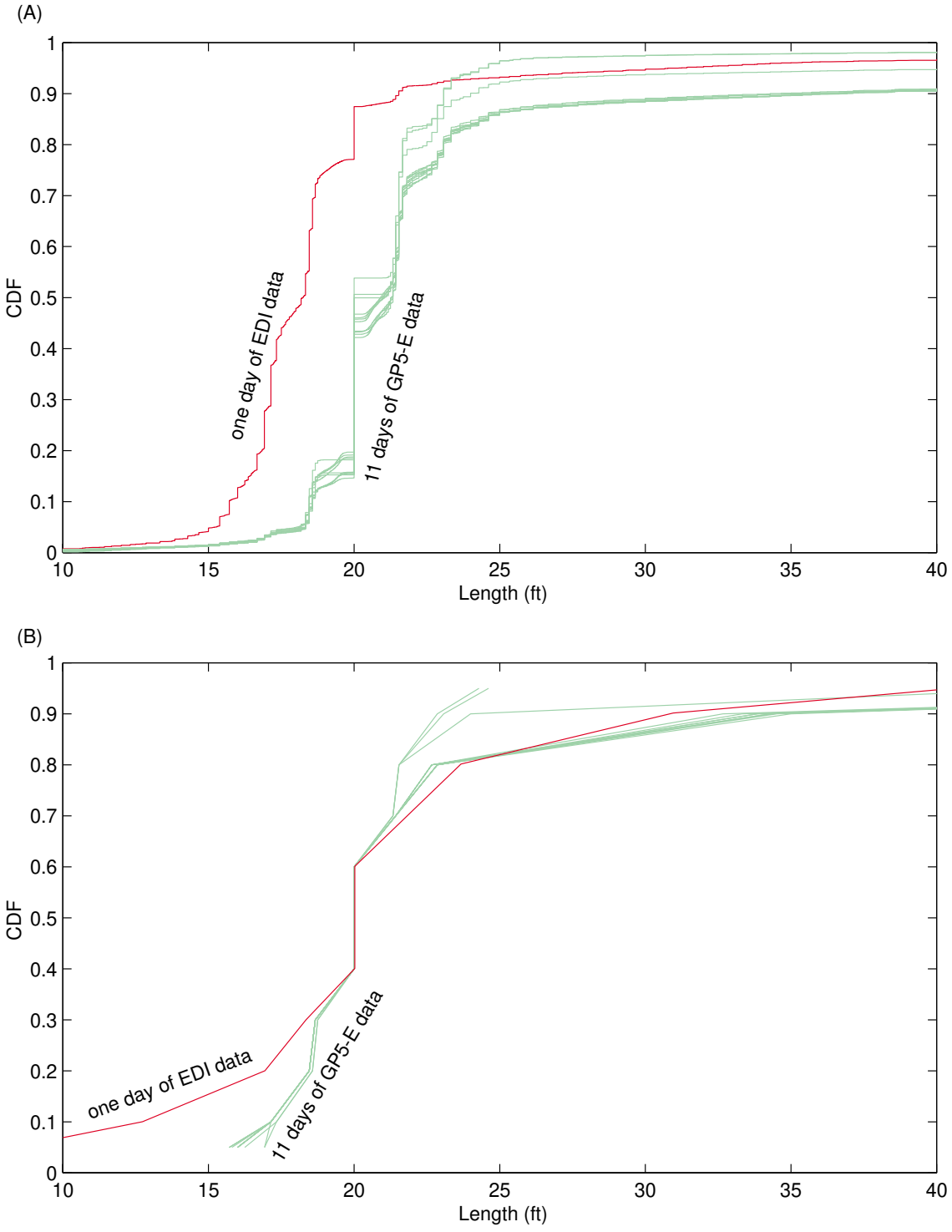

Figure 5-5 (A) Estimated traffic state (high = free flow, low = congested) and measured velocity, (B) distribution of the number of congested samples preceding each free flow sample.

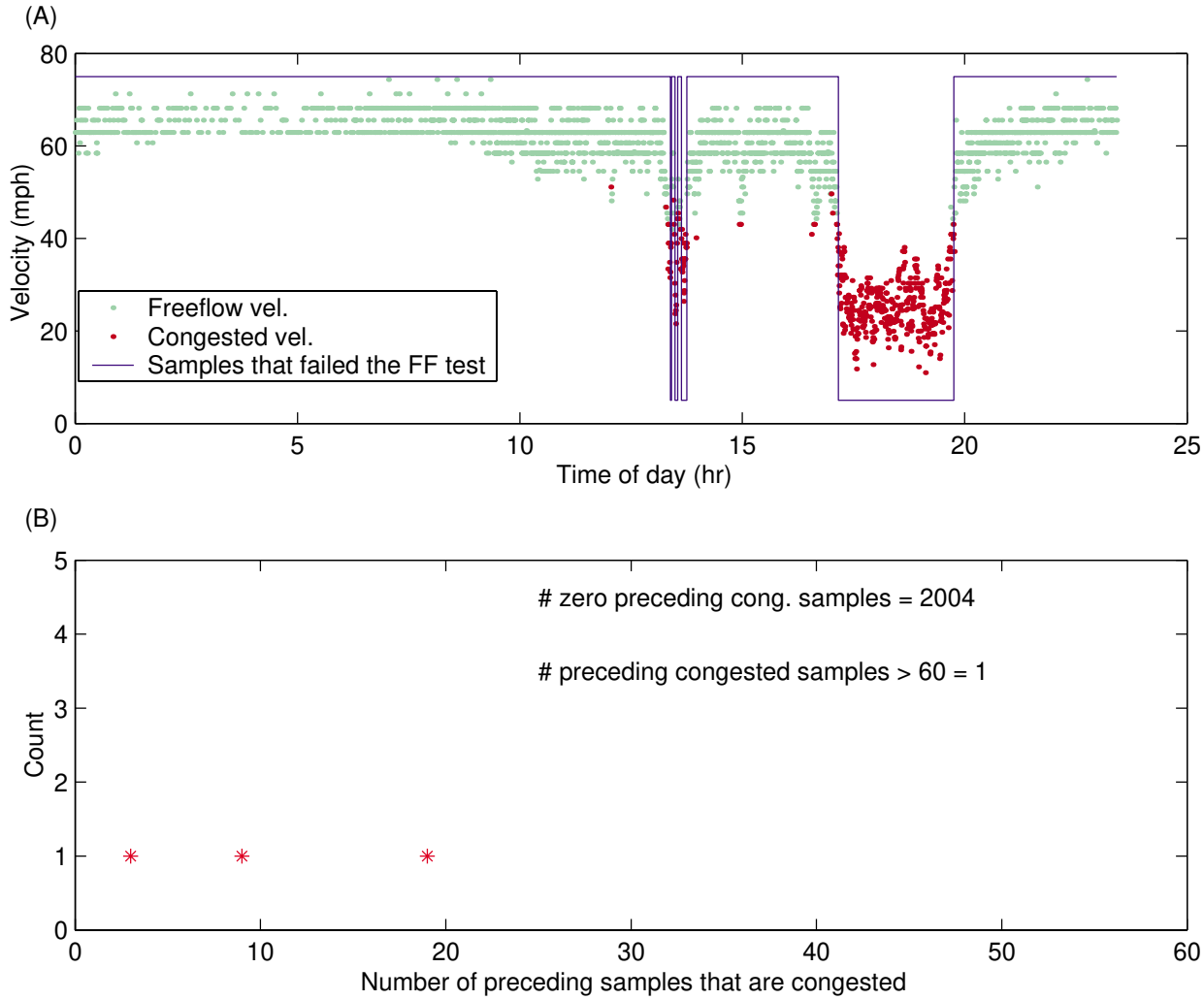

6 REFERENCES

Balke, K., Ullman, G., McCasland, W., Mountain, C., and Dudek, C. (1995) *Benefits of Real-Time Travel Information in Houston, Texas*, Southwest Region University Transportation Center, Texas Transportation Institute, College Station, TX.

Chen, L., and May, A. (1987) Traffic Detector Errors and Diagnostics. *Transportation Research Record 1132*, pp 82-93. Transportation Research Board, Washington, DC.

Cleghorn, D., Hall, F., and Garbuio, D. (1991) Improved Data Screening Techniques for Freeway Traffic Management Systems. *Transportation Research Record 1320*, pp 17-31. Transportation Research Board, Washington, DC.

Coifman, B. (1998) Vehicle Reidentification and Travel Time Measurement in Real-Time on Freeways Using the Existing Loop Detector Infrastructure, *Transportation Research Record 1643*, Transportation Research Board, pp 181-191.

Coifman, B. (1999) Using Dual Loop Speed Traps to Identify Detector Errors, *Transportation Research Record no. 1683*, Transportation Research Board, pp 47-58.

Coifman, B., Lyddy, D., and Skabardonis, A. (2000) The Berkeley Highway Laboratory-Building on the I-880 Field Experiment, *Proc. IEEE ITS Council Annual Meeting*, pp 5-10. Institute of Electrical and Electronics Engineers, Piscataway, NJ.

Coifman, B. (2001) Identifying the Onset of Congestion Rapidly with Existing Traffic Detectors, [submitted for publication].

Coifman, B., and Cassidy, M. (2001) Vehicle Reidentification and Travel Time Measurement on Congested Freeways, [forthcoming].

Courage, K., Bauer, C., Ross, D. (1976) Operating Parameters for Main-Line Sensors in Freeway Surveillance Systems, *Transportation Research Record 601*, pp 19-28. Transportation Research Board, Washington, DC.

Daganzo, C. (1997) *Fundamentals of Transportation and Traffic Operations*, Pergamon.

Dailey, D. (1999) A Statistical Algorithm for Estimating Speed from Single Loop Volume and Occupancy Measurements. *Transportation Research-B*, Vol 33B, No 5, June 1999, pp 313-322. Elsevier Science, London.

Hall, F., Persaud, B. (1989) Evaluation of Speed Estimates Made with Single-Detector Data from Freeway Traffic Management Systems. *Transportation Research Record 1232*, pp 9-16. Transportation Research Board, Washington, DC.

Holemen, B., and Neimeier, D. (1998) Characterizing the Effects of Driver Variability on Real-World Vehicle Emissions, *Transportation Research-Part D*, vol 3, pp 117-128.

Huang, T., and Russell, S. (1997) Object Identification in a Bayesian Context, *Proceedings of the Fifteenth International Joint Conference on Artificial Intelligence (IJCAI-97)*, Nagoya, Japan. Morgan Kaufmann.

Ingram, J. (1976) The Inductive Loop Vehicle Detector: Installation Acceptance Criteria and Maintenance Techniques, California Department of Transportation, Sacramento, CA.

Jacobson, L, Nihan, N., and Bender, J. (1990) Detecting Erroneous Loop Detector Data in a Freeway Traffic Management System. *Transportation Research Record 1287*, pp 151-166. Transportation Research Board, Washington, DC.

Kell, J., Fullerton, I., and Mills, M. (1990) *Traffic Detector Handbook, Second Edition*, Federal Highway Administration, Washington, DC.

Lighthill, M. and Whitham, G. (1955) On Kinematic Waves II. A Theory of Traffic Flow on Long Crowded Roads, *Proc. Royal Society of London, Part A*, vol 229, no 1178, pp 317-345.

Mikhalkin, B., Payne, H., Isaksen, L. (1972) Estimation of Speed from Presence Detectors. *Highway Research Record 388*, pp 73-83. Highway Research Board, Washington, DC.

Nagel, K., Stretz, P., Pieck, M., Leckey, S., Donnelly, R., Barrett, C. (1998) TRANSIMS Traffic Flow Characteristics, paper presented at the 77th annual TRB meeting, Transportation Research Board.

Newell, G. (1993) A Simplified Theory of Kinematic Waves in Highway Traffic, Part II: Queueing at Freeway Bottlenecks, *Transportation Research-Part B*, vol 27, pp 289-303.

Nihan, N. (1997) Aid to Determining Freeway Metering Rates and Detecting Loop Errors. *Journal of Transportation Engineering*, Vol 123, No 6, November/December 1997, pp 454-458.

Palen, J. (1997) The Need for Surveillance in Intelligent Transportation Systems, *Intellimotion*, Vol 6, No 1, University of California PATH, Berkeley, CA, pp 1-3, 10.

Pushkar, A., Hall, F., Acha-Daza, J. (1994) Estimation of Speeds from Single-Loop Freeway Flow and Occupancy Data Using Cusp Catastrophe Theory Model. *Transportation Research Record 1457*, pp 149-157. Transportation Research Board, Washington, DC.

Skabardonis, A., Petty, K., Noeimi, H., Rydzewski, D. and Varaiya, P. (1996) I-880 Field Experiment: Data-Base Development and Incident Delay Estimation Procedures, *Transportation Research Record 1554*, Transportation Research Board, pp 204-212.

Sun, C., Ritchie, S., Tsai, K., Jayakrishnan, R. (1999) Use of Vehicle Signature Analysis and Lexicographic Optimization for Vehicle Reidentification on Freeways, *Transportation Research-Part C*, vol 7, pp 167-185.

Wang, Y., Nihan, N. (2000) Freeway Traffic Speed Estimation Using Single Loop Outputs, paper presented at the 79th Annual Meeting of the Transportation Research Board, Washington, DC.

West, B., McGill, R., Sluder, S., (1999) *Development and Validation of Light-Duty Vehicle Modal Emissions and Fuel Consumption Values for Traffic Models*, Federal Highway Administration.

Windover, J. and Cassidy, M. (2000) Some Observed Details of Freeway Traffic Evolution, *Transportation Research: Part A*, [forthcoming].

Windover, J. (1998) *Empirical Studies of the Dynamic Features of Freeway Traffic*, Dissertation, University of California.